Evaluation of Heterocyclic Aromatic Compound Dye (Methylene Blue) on Chitosan Adsorbent Sourced from African Snail Shell: Modelling and Optimization Studies

Victor Ehigimetor Bello*, Olaosebikan Abidoye Olafadehan
Department of Chemical and Petroleum Engineering, University of Lagos, Akoka-Yaba, Lagos State 101017, Nigeria

Abstract

In this article, the modelling and optimization of five operational process parameters involving initial concentration, adsorbent dosage, contact time, temperature and pH of the solution as it affects the treatment of aqueous solution contaminated with methylene blue, a heterocyclic aromatic compound, on chitosan sourced from African Snail Shell were studied using response surface methodology (RSM) and artificial neural network (ANN) techniques coupled with genetic algorithm. The single and interactive effects of the variables were examined by way of analysis of variance (ANOVA). A comparison of the model techniques was done and an evaluation was carried out with some selected error functions. Both modelling and optimization tools performed creditably well. However, the hybrid ANN-GA proved to be a superior modelling and optimization technique with excellent generalization ability which gave an average absolute deviation $< \pm 3\,\%$ *between the experimental and predicted data of both response variables considered. The insightful relative importance of the process variables based on the renowned Garson and Olden's algorithm methods coupled with step by step approach initiated in the Matlab environment were equally investigated. The findings from this study revealed in clear terms that pH and initial concentrations were the most influential parameters and the maximum value of 99.28% of methylene blue removed at optimum conditions affirmed that the chitosan adsorbent is viable for the treatment of effluents from the textile industry.*

Keywords: *ANOVA, Response Surface Methodology (RSM), Artificial Neural Network (ANN), Genetic Algorithm (GA).*

* Corresponding author. Tel.: +2348066378413
E-mail address: profehisfire@gmail.com

Manuscript History:
Received 13 January, 2022, Revised 10 April, 2022, Accepted 11 April, 2022, Published 30 April, 2022

https://doi.org/10.33736/jaspe.4464.2022

e-ISSN: 2289-7771

1. Introduction

The global community is in dire need of potable water with the standard required to satisfy the demand of the ongoing population boom. Researchers are perturbed about the devastating state of the environment littered with enormous chemical pollutants traced from anthropogenic sources such as industrial activities and natural disasters, characterized by deleterious and severe health problems like breathing problems, vomiting, nausea, asthma, eczema, thyroid cancer, gastritis, diarrhoea, angioedema, etc. [1-3]. Among the myriads of pollutants reported in the literature ravaging the environment mostly the aquatic is the heterocyclic aromatic compound dye compounds such as methylene blue [4-5].

A tremendous amount of dye exists all over the world as natural or synthetic dye mainly used in the food and textile industry respectively. Annually, an estimated amount to the tune of over 7×10^5 tons dyes of 10000 different dyes and pigments are produced and about 200,000 tons are released as wastewater and gaseous substances in the environment [6-9]. The atmospheric environment receives parts of the dye compounds and pigments in the form of gaseous or volatile organic compounds, particulate matter and dust from industrial activities.

More devastatingly, their introduction to the aquatic environment as small as < 1 ppm is highly conspicuous as it affects the aesthetic quality, transparency and solubility of gas [10-12]. Dyes are hazardous, highly toxic and potentially carcinogenic which pose a great threat to human survival and other aquatic organisms. Various animal and human diseases are closely linked or associated with it [13]. In addition, it adversely affects the photosynthesis performance of plants in water bodies by reduction of light penetration [14]. Currently, the immense use of MB in the printing, textile, painting, leather, rubber, pulp and paper, photography, food industries just to mention a few and the unwholesome activities leading to the indiscriminate discharge of effluent to the aquatic environment typifies the sources of this dreadful pollutant adjured from literature to be carcinogenic and mutagenic [15-16].

Nigeria is not out of the knots. Some cities in Nigeria such as Lagos, Kaduna and a few others are still grappling with the menace of effluents from industries of various sectoral classifications. In Lagos state with a population of over 20 million, it accommodates approximately 80% of the industries in Nigeria. The effluents from the textile industry top the list of the negative effect on the environment [16-22]. Against this background, constant efforts by way of government regulations, supervision and monitoring by environmental agencies, and investment through research are ongoing.

Many processes had been explored for wastewater treatment such as filtration, sedimentation, ion exchange, reverse osmosis, precipitation, distillation, flotation, chemical oxidation, ozonation, and electrochemical treatment, as well as adsorption and biological treatment [10,11]. The process of adsorption is preferred among the aforementioned options due to its economic value in terms of cost, simplicity of design, readily available sources of adsorbents with high adherence of pollutants to its active sites and void of sensitivity to toxic substances [23-26].

One of the essential components that influence the efficiency of the adsorption process in wastewater treatment is the nature and adsorption capacity of the adsorbent [27-31]. The pursuit of alternate sources in place of the commercial activated carbon is the foremost interest of environmental researchers. For a few decades, agricultural wastes had undoubtedly been the focus with reports of amazing performance in the treatment of wastewater and had made good of its potential of high adsorption capacity in place of the commercial activated known to be very expensive [27, 31-32]. On account of cost and problems associated with regeneration, researchers have projected the commercial activated carbon to be on a trail to chitosan, a biopolymer and product of the thermo-chemical treatment

of seafood wastes or processing. From literature, it is widely reported as the most abundant linear polysaccharide in nature after cellulose compound [33]. There is increasing snail farming and market in Nigeria [34]. The shell waste site is becoming burdensome to manage since they are non-biodegradable. It has been reported to be a good source of chitosan that can be applied to reduce the impact on the textile industry [35].

Chitosan is made up of (1-4)-linked 2-amino-2deoxy-β-D-glucopyranose [36]. The existence of polar functional groups, hydroxyl (-OH) and –NHR (where R is either H or amide/acetic) in its structural framework gives it its unique adsorption properties [29, 30]. The various modification of chitosan to exhibit properties such as chemical stability, hydrophilicity and a high degree of renewability has equally hyped the use of chitosan as a viable low-cost adsorbent [37].

Aside from the factor of adsorbent, the adsorption process is affected by a number of factors such as initial concentration, adsorbent dosage, pH of the solution, agitation speed, contact time, adsorbent particle size, and operating temperature. The influences of these factors regarding the percentage removal of the concerned pollutant are usually carried out one factor at a time (OFAT) commonly known as the conventional method as populated in the literature. This method is attributed to time consumption, high cost of operation, a laborious number of experimental runs, voidance of predictive ability of the interactive effects of the factors and unreliability of results owing to the fact that the factors are not varied simultaneously [38].

To surmount this hurdle, the use of statistical designs such as the use of Response surface methodology (RSM) have been employed by researchers to model physical processes. Models are extensively used in all facets of science and technology. Modelling is a key enabling tool that aids and enhances the understanding and prediction of the functioning of a process or system predicated on the process or system's principle of operation and material properties [39]. The RSM and ANN are one of reputable modelling techniques cited in the literature [3, 35, 37].

Response surface methodology (RSM) is basically a combination of groups of mathematical and statistical techniques tailored towards the development of an adequate functional relationship between single or multi-response and myriad control variables or factors varied simultaneously [39-41]. The application of RSM in the design, analysis and optimization of processes in various fields of engineering, science and technology attests to its wide acceptance as a useful tool in solving problems involving several independent factors with a great deal of influence on a targeted response variable(s) [40]. The use of RSM as a modelling tool for the treatment of effluent contaminated with MB is often presented in the literature majored in three or four of the highlighted factors [2, 37, 38, 42-58]. Among the arrays of design associated with RSM, the central composite design (CCD) was adopted in this study to accommodate five independent process variables.

The artificial neural network (ANN) technique is an artificial intelligence arm used as an instrument in establishing massive input-output data relationships with proven generalization and high predictive ability whose principle of operation is configured after the biological neural system. Unlike the RSM, the ANN can approximate non-linear functions with the inclusion of quadratic equations without prior knowledge whereas the former is restricted only to second-order polynomial functions [59]. The models developed from ANN are expressed in terms of weights and biases alongside appropriate activation function(s). The use of weights and biases have been previously applied to determine the relative importance of the independent variables involved in any process of interest using algorithms such as Garson's algorithm, Olden' algorithm, etc. commonly used in environmental or ecological studies

[60]. In addition, they have been used to develop empirical equations which have reasonably demystified the black box character associated with ANN as a modelling tool [61].

The choice of RSM-fractional central composite design is influenced by the advantage it affords which is essentially the ability to generate an experimental matrix with relatively few runs, ultimately saving time, energy and valuable resources. On the other hand, the use of ANN somewhat guarantees superior modelling ability for complex non-linear relationships among the input and output data embedded in any experimental design as provided by RSM [62].

Another vital aspect of modelling is the optimization of the parameters associated with any process or system for effective performance. Optimization is geared toward determining the optimal values of process parameters that match the desired response or output value [63]. An evolutionary algorithm is very much in application in achieving optimal conditions since it is not subject or prone to a local minimum or maximum entrapment contrariwise to response surface methodology and artificial neural network (ANN). Such evolutionary algorithms include genetic algorithm (GA), simulated annealing (SA), and particle swarm optimization among others.

The purpose of this study is to model the adsorption process using RSM and ANN techniques; compare the degree of accuracy of both techniques; optimize the influencing factors (initial concentration, solution pH, temperature, adsorbent dosage and contact time) of the adsorption process with the aid of RSM-GA and ANN-GA hybrid; ascertain the relative importance of the factors using the analysis of variance (ANOVA) result associated with RSM and the Garson algorithm, olden algorithm and step-by-step approach common with ANN. To the best of our knowledge, no study has delved into the aforementioned objectives of this study, precisely the treatment of aqueous solution contaminated with methylene blue with the use of chitosan extracted from African snail shells.

2. Materials and Methods

2.1. Materials

The chemical reagents used in this study were all analytical grade and they were used without prior treatment viz: (i) Methylene blue ($C_{16}H_{18}N_3SCl$-molecular weight of 319.85 g/mol and 98.7% purity), (ii). NaOH pellet (99.8% purity) and (iii) HCl (36.5-38 %, sp. gr. 1.18) were purchased from Loba Chemie PVT Limited (India), Merck and BDH Laboratories Supplies, England respectively.

2.2.2 Adsorbent characterization

The physiochemical properties of the chitosan adsorbent were characterized to ascertain the degree of deacetylation, moisture content, ash content, molecular weight, protein content, FT-IR, Surface Morphology using SEM, the crystalline nature using XRD.

2.2.3 Preparation of adsorbate

A stock solution of 1000 mg/L of methylene blue (MB) was prepared by dissolving a weighed portion of 1 g of it in 1000 cm^3 (or 1 L), from which various concentrations were obtained by serial dilution.

2.2.4 Batch Adsorption Experiment

The batch adsorption of methylene blue (MB) on the chitosan flakes was designed using Central Composite Design comprising five variables: Initial concentration (20-100mg/l), adsorbent dosage (0.25-1.25g), contact time (15-75min), temperature (35-95^{o}C) and pH (3-11) as depicted in Table 1. The experimental design which consists of sets of experimental runs was generated using a Design expert under different conditions described in Table 2. The batch adsorption was contained in a 250 ml capacity of Erlenmeyer flasks placed on a magnetic stirrer built with a temperature-controlled device. The pH values were obtained by dropwise addition using 0.1 M HCl and 0.1 M NaOH measured by a pH meter. The solutions were filtered after the designated contact time using Whatman filter paper (No. 42) and the residual concentration was determined using an ultra-visible spectrophotometer λ_{max} of 650nm.

2.3 Optimization Tools

Response Surface Methodology (RSM), Artificial Neural Network and Genetic algorithm were used for the optimization process.

2.3.1 Response Surface Methodology (RSM)

The Response Surface Methodology (RSM) is one the most reliable tools to process engineers in determining optimum conditions, maximum amount and insightful interaction analysis of various operational variables of a given process at a relatively significant reduced experimental time and cost in terms of personnel and materials [39]. The removal efficiency (%) and adsorption amount (mg/g) of MB on the chitosan flakes were considered as the response variables of the system for RSM analysis. This optimization technique model the process using the second-order quadratic model to relate the relationship between the responses and the independent variables. Generally, it is expressed as:

$$Y = \beta_0 + \sum_{i=1}^{k} \beta_i X_i + \sum_{i=1}^{k} \sum_{j=1}^{k} \beta_{ij} X_i X_j + \sum_{i=1}^{k} \beta_{ii} X_{ii}^{\ 2} + 1 \quad (1)$$

Where Y represents the responses (dependent variable), β_o is the constant coefficient, β_i, β_{ii}, β_{ij} are coefficients for linear, quadratic interaction effects, respectively, X_i and X_j are the independent variables or factors.

2.3.2 Experimental Design

For the optimization of the conditions of MB adsorption on chitosan flakes, the fractional Central Composite Design (CCD) was employed to design the experiment involving five independent variables: initial concentration, adsorbent dosage, contact time, temperature and pH denoted as X_1, X_2, X_3, X_4 and X_5 using design expert version 12 (trial version). The full CCD consists of 2^n factorial runs, with $2n$ axial runs and n_C centre runs. The number of experimental runs is evaluated given the expression [67-68]:

$$N = 2^n + 2n + n_c \quad (2)$$

However, for a fraction of CCD, the 2^n factorial runs become 2^{n-1} runs. Thus, equation (2) becomes:

$$N = 2^{n-1} + 2n + n_c \quad (3)$$

Table 1: Coded and uncoded factors for the design of experimental range and levels

Control factors	-α(-2)	-1	0	1	+α (+2)
Initial concentration, X_1 (mg/L)	20	40	60	80	100
Adsorbent dosage, X_2 (g)	0.25	0.5	0.75	1	1.25
Contact time, X_3 (Min)	15	30	45	60	75
Temperature, X_4 (ºC)	35	50	65	80	95
pH, X_5	3	5	7	9	11

Table 2: Experimental design generated by Design-Expert version 12 for the adsorption of MB

Experimental Runs (Standard Order)	X_1	X_2	X_3	X_4	X_5
1	40	0.5	30	50	9
2	80	0.5	30	50	5
3	40	1	30	50	5
4	80	1	30	50	9
5	40	0.5	60	50	5
6	80	0.5	60	50	9
7	40	1	60	50	9
8	80	1	60	50	5
9	40	0.5	30	80	5
10	80	0.5	30	80	9
11	40	1	30	80	9
12	80	1	30	80	5
13	40	0.5	60	80	9

14	80	0.5	60	80	5
15	40	1	60	80	5
16	80	1	60	80	9
17	20	0.75	45	65	7
18	100	0.75	45	65	7
19	60	0.25	45	65	7
20	60	1.25	45	65	7
21	60	0.75	15	65	7
22	60	0.75	75	65	7
23	60	0.75	45	35	7
24	60	0.75	45	95	7
25	60	0.75	45	65	3
26	60	0.75	45	65	11
27	60	0.75	45	65	7
28	60	0.75	45	65	7
29	60	0.75	45	65	7
30	60	0.75	45	65	7
31	60	0.75	45	65	7
32	60	0.75	45	65	7

The fractional experiment runs consist of 32 runs with 16 factorial, 10 axial (to determine experimental error) and 6 centre points (to ensure constant variance in model prediction). For five factors fractional CCD with alpha value, $\alpha = \pm 2$ (obtained from $\alpha = (2^{n-1})^{0.25}$) [68], the minimum and maximum values correspond to the range of values considered when the operational single factor effects were carried out as reported by Olafadehan et al., 2022 [69].

Table 1 depicts the coded and uncoded independent variables values within the purview of the experimental range and levels. The coded values were obtained using the relationship:

$$X_i = \frac{2[2X - (X_{max} + X_{min})]}{X_{max} - X_{min}} \quad \text{……..} \quad (4)$$

where X_i is the required coded values of a variable X, X is any value of the variable from X_{min} to X_{max}, X_{min} is the lower level of the variable and X_{max} is the upper level of the variable.

Table 2 shows the uncoded experimental design for the optimization of MB on the chitosan flakes under 5 input variables of initial concentration, adsorbent dosage, contact time, temperature and pH denoted as also as X_1, X_2, X_3, X_4 and X_5 respectively. The procedures involved in the use of RSM are shown in Figure 1.

2.3.3 Artificial Neural Network (ANN)

The artificial neural network is an optimization technique capable of performing a nonlinear mapping between inputs and outputs with prior minimal knowledge of the system using computational procedures that simulate the neurological processing ability of the human brain [70-71]. It is widely reported to be characterized by three distinct layers (input, hidden and output) as shown in Figure 2,

consisting of neurons interconnected essentially by the nonlinear activation transfer function(s) like tansig, purelin and sigmoidal with peculiar weights and bias obtained via the application of learning algorithms [59]. The transfer functions could be any one or combination of the following [72-73].

The hyperbolic tangent sigmoid transfer function (tansig):

$$F_i = \frac{2}{1+e^{-2x}} - 1,\ -1 \le F_i \le 1 \quad (5)$$

Sigmoidal transfer function:

$$F_i = \frac{1}{1+e^{-x}},\ 0 \le F_i \le 1 \quad (6)$$

Purelin (Linear): $F_i = x,\ -\infty \le F_i \le +\infty$ (7)

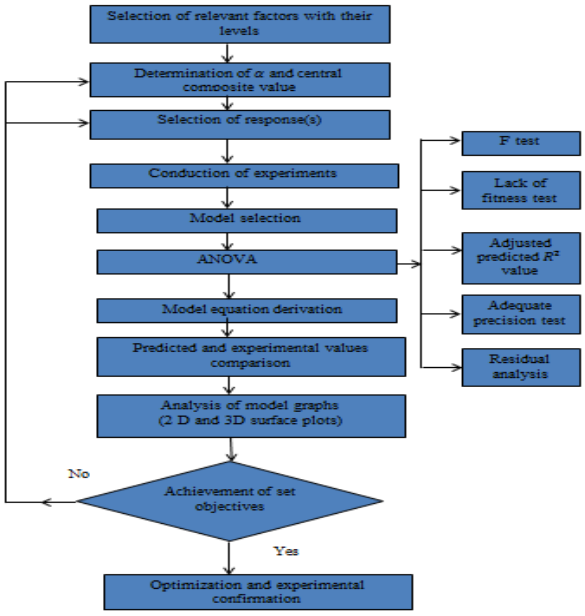

Figure 1: Flowchart of response surface methodology.

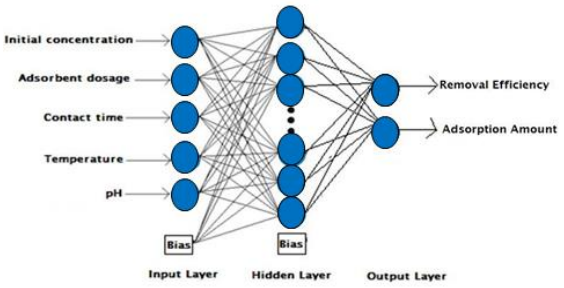

Figure 2: Description of the Artificial Neural Network

2.3.4 Genetic Algorithm

The genetic algorithm is the most evolutionary algorithm pioneered by Goldberg and John Holland. It leverages on the principle of genetic and natural selection. It is basically a heuristic and searches inclined technique applied to solve a myriad of simple and complex problems by seeking possible optimal solutions [74]. Its operation entails 4 major steps as captured in Figure 4. The algorithm begins with a set of individuals tagged as a population presumed to be a possible solution. Each individual in the population pool is assigned a fitness value based on the objective function. Evaluation of individuals' fitness followed sort. Those with satisfactory values transcend to the next phase of crossover, recombination and mutation. The iterative cycle is maintained until the desired solution is reached before termination. The algorithm can be implemented in a Matlab environment [74-78].

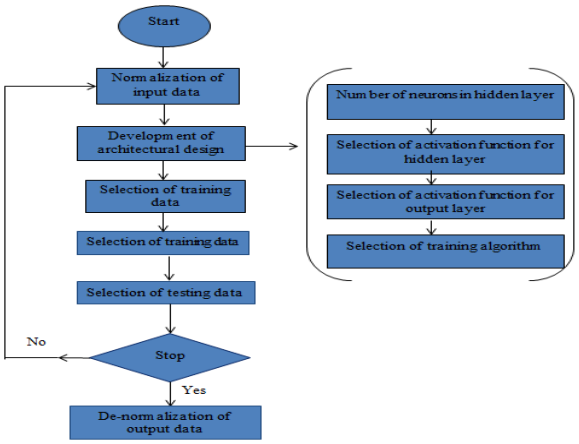

Figure 3: Flowchart of Artificial Neural Network

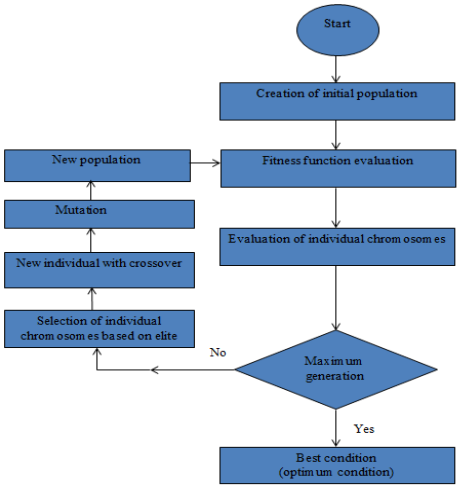

Figure 4: Flowchart of Genetic Algorithm

3. Results and Discussion

3.1 Characterization

Earlier modelling, optimization of the extraction process and characterization of the adsorbent (Chitosan flakes) from African Giant snail by the same authors Bello and Olafadehan [35] revealed the results captured in Table 3. Equally reported exhaustively are the morphology, elemental analysis, functional group and crystalline nature of the adsorbent (before and after adsorption of MB), which was carried out using Scanning Electronic Morphology (SEM), Electron Dispersive X-ray Spectroscopy (EDS), Fourier transform infrared spectroscopy (FT-IR) and X-ray diffraction (XRD) respectively.

Table 3: Physicochemical properties of adsorbent (chitosan) prepared from African snail shell

MC (%)	AC (%)	Fibre content (%)	Protein content (in acetic acid)	Viscosity @ 20 °C (cP)	Molecular weight (g/gmol)	bulk density (g/cm^3)	pHpzc	% DD
5.50	0.25	2.70	0.85 ± 0.27	85.20	2.2×10^5	0.9	7.8	83.10

3.2 Response Surface Methodology

After the elimination, some insignificant terms using the backward elimination technique option as provided by the design expert software version 12.0, the hierarchically maintained quadratic model in terms of actual factors for the removal efficiency of MB (%) and adsorption capacity (mg/g) of the chitosan flakes whose coefficients were estimated respectively:

$$Y_{re} = 84.16207 + 0.682072X_1 - 0.147913X_3 - 0.527906X_4 - 1.88705X_5 - 0.005620X_1.X_3 - 0.037007X_4.X_5 - 0.002053{X_1}^2 + 0.005902{X_3}^2 + 0.006552{X_4}^2 + 0.310787{X_5}^2$$

……(8)

$$Y_{qe} = 1.35820 + 0.095267X_1 - 0.725146X_2 - 0.013426X_3 - 0.042714X_4 - 0.042489X_5 - 0.000270X_1.X_3 + 0.011696X_2.X_4 - 0.001754X_4.X_5 + 0.000127{X_1}^2 + 0.000344{X_3}^2 + 0.000383{X_4}^2 + 0.010554{X_5}^2$$

…….(9)

Table 4 shows that the model equations are characterized by a coefficient of determination, R^2 of 0.8680 and 0.9988 for efficiency removal and adsorption amount respectively. This implies that 13.2% and 0.12% of the total variation could not be explained, i.e the proportion of variance in the dependent variables that are not predictable from the independent variables. The closeness of the adjusted coefficient of determination, ${R^2}_{adj}$ of 0.8052 and 0.9980 to their respective values of coefficient of

determination, R^2 is a slight difference of less than 0.2 which is a good indication of the fitness of the model.

It is imperative to note that Adeq Precision, indices that measure the signal to noise ratio was evaluated as 16.7718 and 157.6535 for both responses which are far greater than 4 and are within the desirable limit. This result posits the propriety of the models in navigating the design space.

The regression model's F-values of 13.81 and 1271.68 for the response variables translate that the model is significant. This establishes respectively the fact that only 35.31% and 93.34% chance these F-values this large could occur as a result of noise. Furthermore, the insignificant lack of 0.3531 and 0.9334 in Tables 5 and 6 for removal efficiency and adsorption amount respectively implies that it is not significant with respect to the pure errors [44,79]. P-values less than 0.0500 indicate model terms are significant while values greater than 0.1000 mean that the model terms are not significant.

It is worthy of note that for removal efficiency of MB on chitosan flakes, initial concentration (X_1) and temperature (X_4) are the only significant linear terms; initial concentration (X_1^2), contact time (X_3^2), temperature (X_4^2) and pH (X_5^2) are the only significant quadratic terms, and the significant interactive terms are initial concentration and contact time ($X_1.X_3$), temperature and pH ($X_4.X_5$) as presented in Table 5.

Similarly in Table 6, for adsorption amount, initial concentration (X_1) and temperature (X_4) are the only linear significant terms; initial concentration (X_1^2), contact time (X_3^2) and pH (X_5^2) are the only quadratic terms that are significant and initial concentration and contact time ($X_1.X_3$), adsorbent dosage and temperature ($X_2.X_4$), temperature and pH ($X_4.X_5$) are the only significant interactive terms. In these regards, equations 8 and 9 prediction ability can be certain to be very high.

Equation 8 indicated that all single terms have an antagonistic effect on the response variables except for the initial concentration which has a synergistic effect. All square terms have positive effects except for adsorbent dosage with a negative effect and the interaction terms of initial concentration and contact time ($X_1.X_3$) and temperature and pH ($X_4.X_5$) have an antagonistic effect on the response variables. In a similar development, equation 9 shows that the initial concentration reflects a positive effect while all other single terms produce a negative effect on the adsorption amount. All square terms in the equation depict positive effects and the interactive terms of initial concentration and contact time ($X_1.X_3$) and temperature and pH ($X_4.X_5$) also indicate a negative influence on adsorption amount. The implication is that antagonist factors that change from the minimum to maximum levels will lead to a decrease in response variables. Conversely, synergistic factors result in a positive effect on the response variables [80].

Table 4: Statistical fits values for removal efficiency model and adsorption capacity equation

	Removal Efficiency (%)	**Adsorption Capacity (mg/g)**	**Statistical parameters**	**Removal Efficiency (%)**	**Adsorption Capacity (mg/g)**
Std. Dev.	2.08	0.0783	R^2	0.8680	0.9988
Mean	88.78	5.370	Adjusted R^2 (R^2_{adj})	0.8052	0.9980
C.V. %	2.340	1.460	Predicted R^2	0.6071	0.9970

PRESS	270.12	0.2766	Adeq Precision	16.7718	157.6535

Table 5: Analysis of variance (ANOVA) for removal efficiency of MB

Source	Sum of Squares	Df	Mean Square	F-value	p-value	
Model	596.80	10	59.68	13.81	< 0.0001	Significant
X_1	320.93	1	320.93	74.29	< 0.0001	
X_3	11.47	1	11.47	2.66	0.1181	
X_4	22.66	1	22.66	5.24	0.0325	
X_5	0.3290	1	0.3290	0.0762	0.7853	
$X_1.X_3$	45.47	1	45.47	10.53	0.0039	
$X_1.X_5$	19.72	1	19.72	4.56	0.0446	
X_1^2	19.92	1	19.92	4.61	0.0436	
X_3^2	52.09	1	52.09	12.06	0.0023	
X_4^2	64.19	1	64.19	14.86	0.0009	
X_5^2	45.65	1	45.65	10.57	0.0038	
Residual	90.72	21	4.32			
Lack of Fit	74.88	16	4.68	1.48	0.3531	not significant
Pure Error	15.85	5	3.17			
Cor Total	687.52	31				

Figure 5a-b reflects the investigation of the normality of the data. The plots reveal that the errors are distributed since the residuals are located on or close to the straight line. The independency of the data was also examined by the plot shown in Figure 6a-b, that is, the plot of the residuals and the run order for removal efficiency (%) and adsorption capacity (mg/g) respectively. The figures clearly show that patterns formed are not in predictable form within the levels of -3 to 3. The extent of correlation between the predicted values and the experimental values (actual values) is described in Figures 7a-b. Due to the alignment of data along the straight line, it can be inferred that a good agreement existed for both response variables [81].

The combined effect of initial concentration and contact time on the percentage removal of MB and the adsorption amount is depicted in Figures 8a-b and 9a-b respectively. The plots reveal that as both control factors increase 40-80mg/L and 30-60min respectively, the responses increase accordingly. A similar trend was observed for initial concentration and temperature as shown in Figures 10a-b and 11a-b as factors progress respectively from 40-80mg/L and 30-80^{o}C which bring about an increase in the percentage of MB and adsorption amount. Figure 12a-b and 13a-b vividly illustrate the results that are associated with the interaction of temperature and pH on both responses. A steady increase in the responses was observed as the independent variables increase from the temperature value of 30-80^{o}C and solution pH of 3-11. The sharp increase of the responses was immediately above the pH value of 7 because of the points of zero charge value of the adsorbent, pHpzc. Solution pH above pHpzc averts protonation of the adsorbent surface facilitates electrostatic attraction of MB molecules to the active site

of the adsorbent [44, 54, 69]. The increase in temperature may have enhanced the movement of the MB molecules and improved diffusion to the active sites

Table 6: Analysis of variance (ANOVA) for adsorption capacity of chitosan flakes

Source	Sum of Squares	Df	Mean Square	F-value	p-value	
Model	93.64	12	7.80	1271.68	< 0.0001	significant
X_1	92.94	1	92.94	15145.79	< 0.0001	
X_2	0.0018	1	0.0018	0.3010	0.5897	
X_3	0.0087	1	0.0087	1.410	0.2492	
X_4	0.0665	1	0.0665	10.83	0.0038	
X_5	0.0074	1	0.0074	1.200	0.2863	
$X_1.X_3$	0.1053	1	0.1053	17.17	0.0006	
$X_2.X_4$	0.0308	1	0.0308	5.020	0.0373	
$X_4.X_5$	0.0443	1	0.0443	7.220	0.0146	
X_1^2	0.0768	1	0.0768	12.51	0.0022	
X_3^2	0.1765	1	0.1765	28.77	< 0.0001	
X_4^2	0.2188	1	0.2188	35.66	< 0.0001	
X_5^2	0.0526	1	0.0526	8.580	0.0086	
Residual	0.1166	19	0.0061			
Lack of Fit	0.0595	14	0.0043	0.3728	0.9334	not significant
Pure Error	0.0570	5	0.0114			
Cor Total	93.760	31				

Within the range studied, the increase of initial concentration and that of adsorbent dosage as they interact gave a non-significant effect on the responses due to saturation of the active sites or aggregation formation resulting in high resistances caused by mass transfer against diffusion from the bulk to the surface active sites; decrease in intercellular distances; high screening effect and protection of the adsorption sites of the chitosan adsorbent. This was also corroborated by the 2D plot with the contour plot marked with parallel lines and void of curvature [56, 82-83].

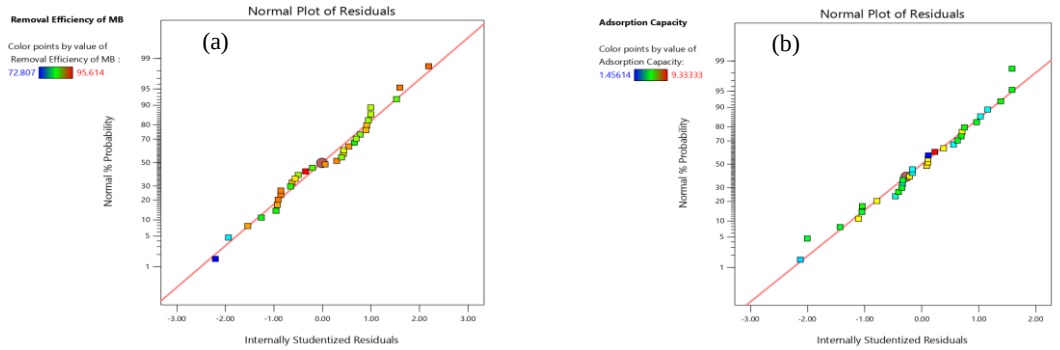

Figure 5: Normality plot of (a) removal efficiency; and (%) (b) adsorption capacity (mg/g)

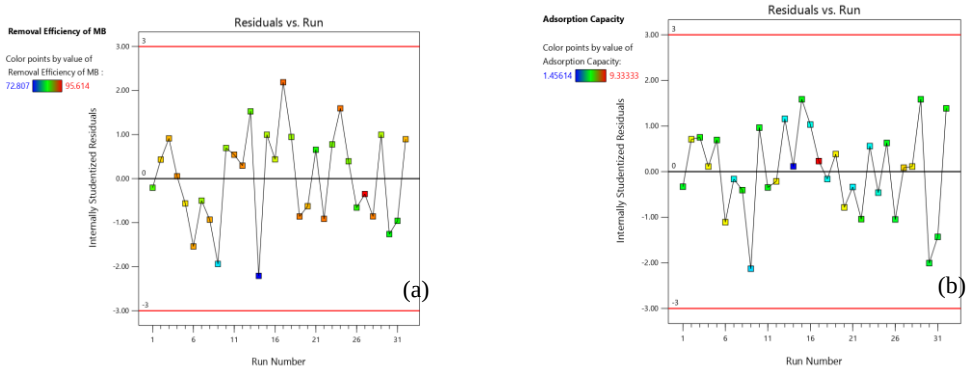

Figure 6: Residual plot of: (a) percentage removal (%); and (b) adsorption capacity (mg/g)

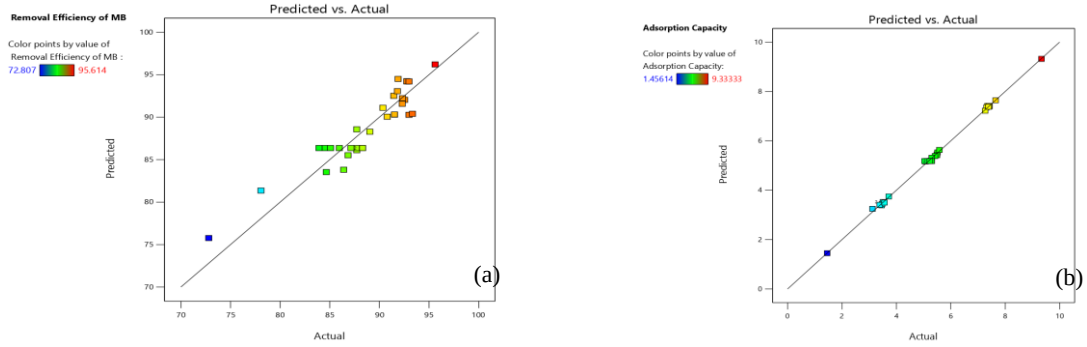

Figure 7: Plot of predicted values versus actual values of (a) percentage removal (%) and (b) adsorption capacity (mg/g)

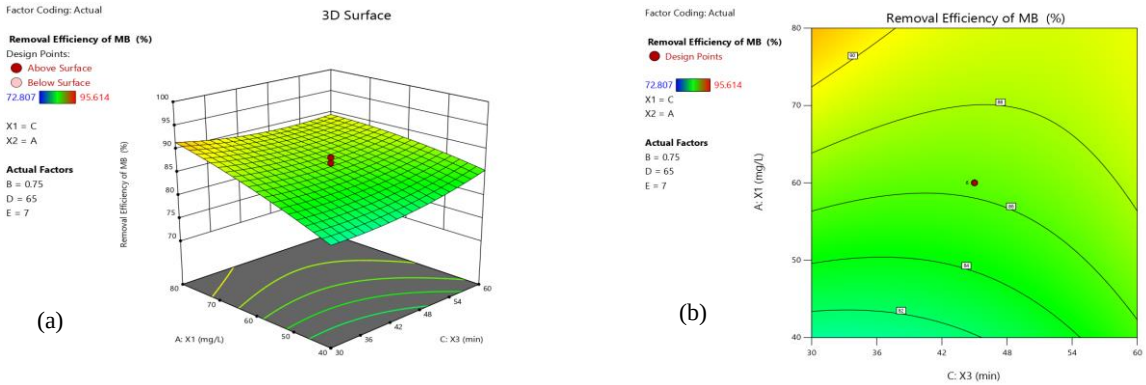

Figure 8: Response surface plot of removal efficiency (a) 3D; and (b) 2D of Initial concentration and contact time at constant adsorbent dosage (0.75g), temperature (65ºC) and pH (7).

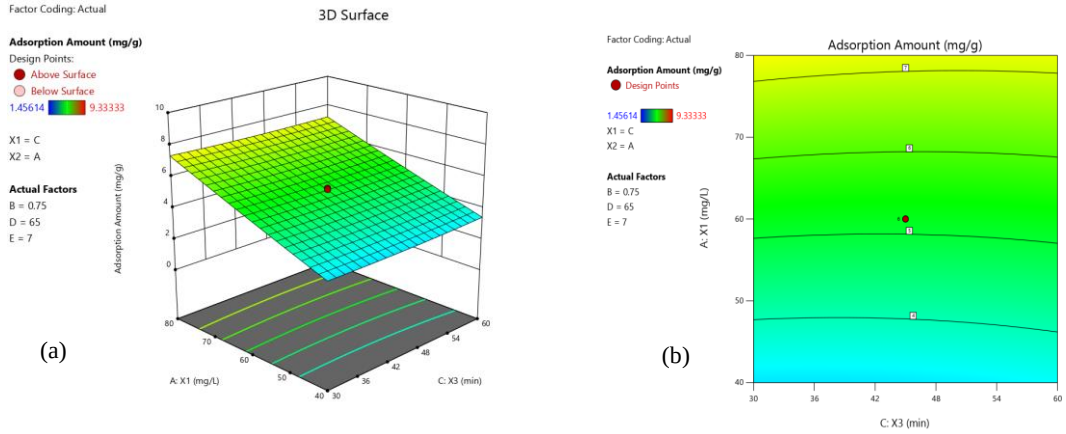

Figure 9: Response surface plot of adsorption capacity (a) 3D; and (b) 2D of Initial concentration and contact time at constant adsorbent dosage (0.75g), temperature (65ºC) and pH (7).

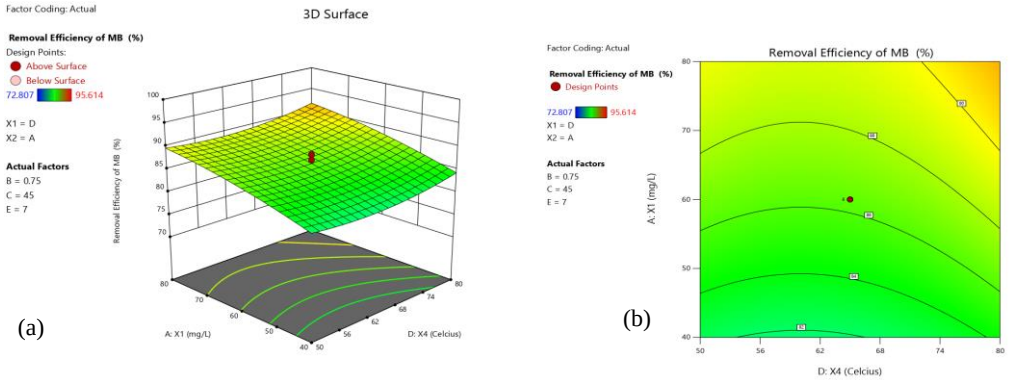

Figure 10. Response surface plot of percentage (a) 3D (b) 2D of initial concentration and temperature at constant adsorbent dosage (0.75g), contact time (45min) and pH (7).

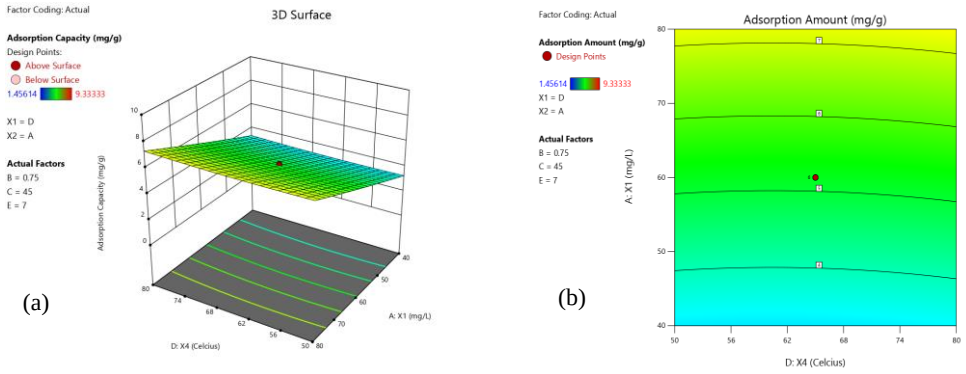

Figure 11. Response surface plot of adsorption capacity (a) 3D; and (b) 2D of initial concentration and temperature at constant adsorbent dosage (0.75g), contact time (45min) and pH (7).

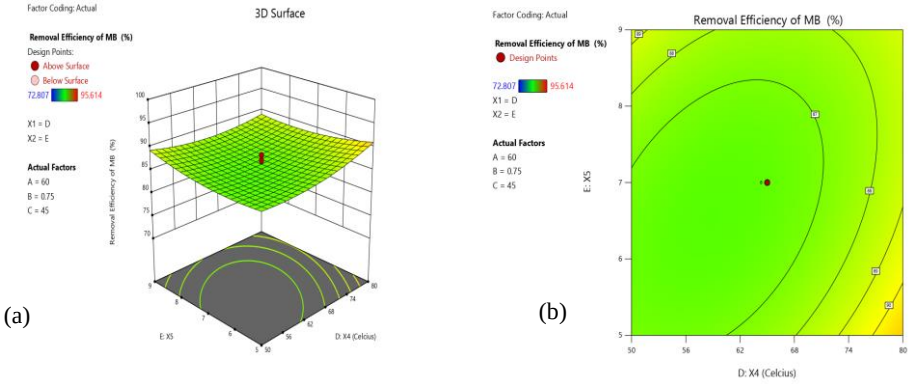

Figure 12. Response surface plot of percentage removal (a) 3D; and (b) 2D of temperature and pH at constant initial concentration (60mg/l), adsorbent dosage (0.75g) and contact time (45min).

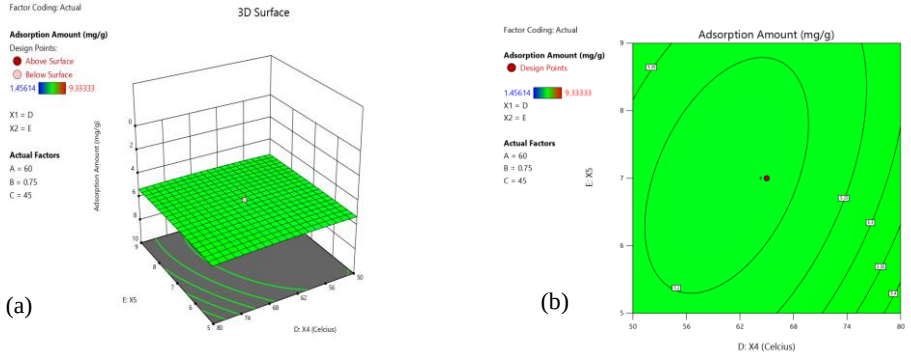

Figure 13. Response surface plot of adsorption capacity (a) 3D; and (b) 2D of temperature and pH at a constant initial concentration (60mg/l), adsorbent dosage (0.75g) and contact time (45min).

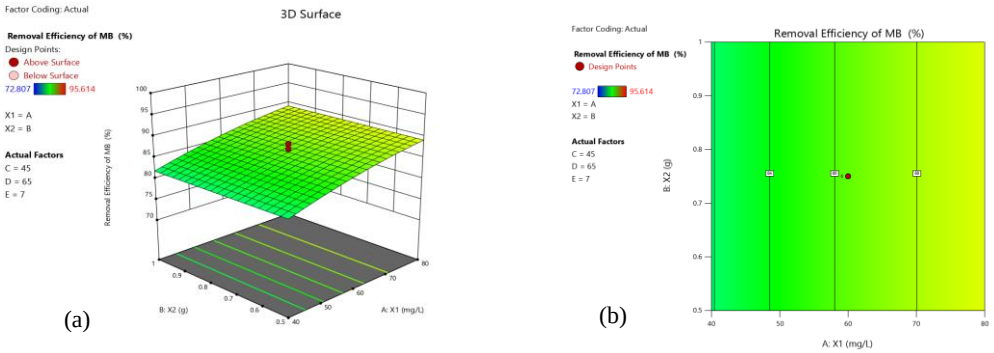

Figure 14. Response surface plot of removal efficiency (a) 3D; and (b) 2D of initial concentration and adsorbent dosage at constant contact time (45min), temperature (65^{o}C) and pH (7).

The Pareto analysis of the parameters was carried out with the intent to examine the relative importance of the parameters according to the equation [84-85]:

$$P_i = \left(\frac{b_i^2}{\sum b_i^2} \right) \times 100 \qquad (10)$$

Where bi represents the coefficients of each parameter in the model equation developed from RSM. Using equations 8 and 9, the results are captured in Table 7. The result reveals that solution pH, X_5 and adsorbent dosage, X_2 are the most influential parameters for percentage removal and adsorption amount respectively.

Table 7: Relative importance of parameters based on RSM model equation

Percentage removal			Adsorption amount		
Parameters	**Relative importance (%)**	**Ranking**	**Parameters**	**Relative importance (%)**	**Ranking**
X_1	10.5139	2	X_1	1.6839	2
X_3	0.4944	5	X_2	97.5625	1
X_4	6.2983	3	X_3	0.0334	5
X_5	80.4770	1	X_4	0.3385	3
X_1X_3	0.0007	9	X_5	0.3350	4
X_4X_5	0.0310	6	X_1X_3	1.35E-05	11
X_1^2	9.53E-05	10	X_2X_4	0.0254	6
X_3^2	0.0008	8	X_4X_5	0.0006	8
X_4^2	0.0010	7	X_1^2	2.99E-06	12

X_5^2	2.1829	4	X_3^2	2.2E-05	10
			X_4^2	2.72E-05	9
			X_5^2	0.0207	7

3.3 Artificial Neural Network

The design of ANN architecture was optimized to get the appropriate algorithm with the right transfer function or combination of functions by checking for the one with the least MSE error function value as depicted in Figure 16, which gives the optimized ANN Architecture Properties shown in Table 8. The Bayesian regularization (BR) algorithm was found to be the best algorithm with the least minimum mean square error for the adsorption amount of MB adsorbed on chitosan flakes response while the Levenberg Marquardt algorithm was the best for removal efficiency of MB by the chitosan flakes. Prior to obtaining the appropriate design or topology, the data were normalized to avoid ill-conditioning arising from large inputs using the mapminmax function given as [35]:

$$X_{norm} = 2\left(\frac{X_i - X_{\min}}{X_{\max} - X_{\min}}\right) - 1 \tag{11}$$

Where X_i is the input data, $X_{\min}$ and $X_{\max}$ are the respective minimum and maximum values of variables X.

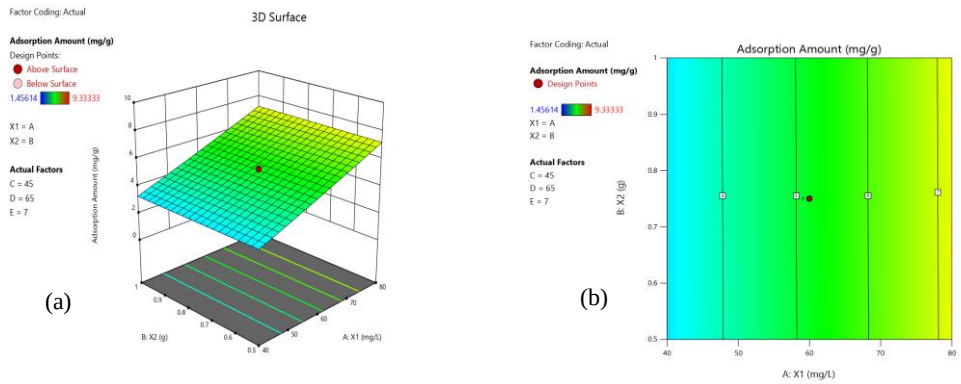

Figure 15. Response surface plot of adsorption amount (a) 3D; and (b) 2D of initial concentration and adsorbent dosage at a constant time (45min), temperature (65°C) and pH.

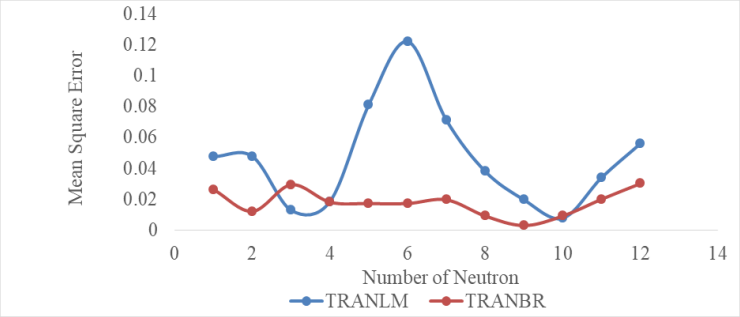

Figure 16: Plot of mean square error (MSE) versus the number of neurons for optimized ANN architecture

Table 8: Optimized ANN architecture properties

Output (Responses)	Network type: Feed Forward Backpropagation Adaptation Learning function: LEARNGDM Performance function: MSE Training Algorithms	Input Layer No. of Neurons	Hidden Layer No. of Neurons	Hidden Layer Activation Function	Output Layer No. of Neurons	Output Layer Activation Function
Adsorption Amount (mg/g)	Bayesan Regularization Backpropagation (TRAINBR)	5	9	Hyperbolic Tangent Sigmond (Transig)	1	Linear (Purelin)
Removal efficiency (%)	Levenberg Marquardt (TRAINLM)	5	10		1	

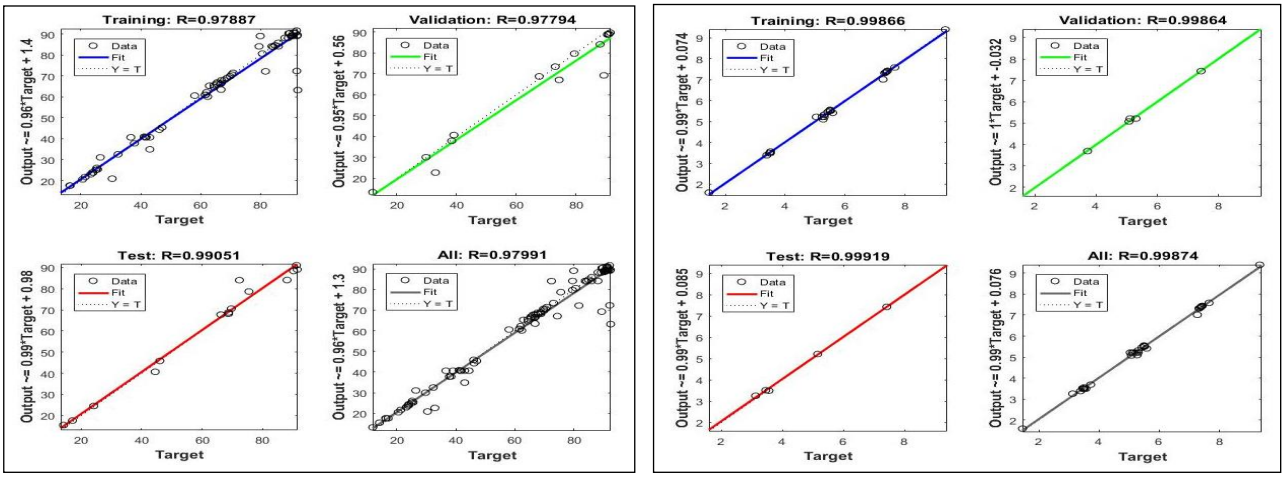

(a) (b)

Figure 17: Plot of training, validation, test and overall regression for adsorption amount of (a) removal efficiency; and (b) adsorption amount.

Figure 17 shows the product of the outcome of the ANN topology leading to training of 0.97887 and 0.99866, validation value of 0.97794 and 0.99864, 0.99051 and 0.99919 test value and overall coefficient of determination of 0.97991 and 0.99874 for both responses. The best validation plot in Figure 18 usually presented in terms of MSE in a log scale format, describes the training process as the ANN technique fits the data through a number of iterations or epochs [86]. From the trend in Figure 18, the training terminates after 4 and 3 iterations for percentage removal and adsorption amount respectively before maintaining a certain low MSE value. The overall MSE value reads an appreciably successful training process with an approximated low value of 0.0040 and 0.0016 for both responses respectively.

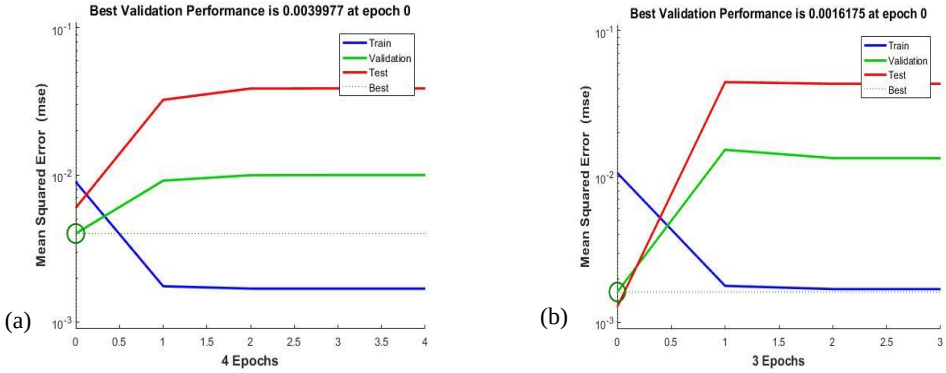

Figure 18: Mean square error (MSE) and the number of iterations (Epochs) performance plot for (a) percentage removal and (b) adsorption amount.

3.4 Sensitivity Analysis

Using the results of the weights and bias generated at the optimized ANN network presented in Table 9 and Table 10, sensitivity analysis to evaluate the relative importance of the independent variables was initiated using the Garson's algorithm and Olden's algorithm expressed respectively as [35, 87-88]:

$$R_{ij} = \frac{\sum_{j=1}^{n_H}\left(i_{vj}\Big/\sum_{k=1}^{n_v} i_{kj}\right)O_i}{\sum_{i=j}^{n_V}\left[\sum_{j=1}^{n_H}\left(i_{vj}\Big/\sum_{k=1}^{n_V} i_{kj}\right)O_j\right]} \tag{12}$$

where R_{ij} is the relative importance of the variable X_i with respect to the output neurons j, n_V is the number of inputs neurons, n_H the number of hidden neurons, i_j the absolute value of connection weights between the inputs, O_j is the connection weight between the inputs values (i) and hidden neurons (j) values and the hidden layers, O_i is the absolute value of connection weights between the hidden and output layers.

$$R_{ij} = \sum_{H=1}^{K} W_{ik} \times W_{kj} \tag{13}$$

where H is the number of neurons in the hidden layer, W_{ik} is the synaptic connection weight between the input neuron i and the hidden neuron k, W_{kj} is the synaptic weight between the hidden neuron k.

Table 9: Weights and bias in input-hidden layers (W_i and b_i) and hidden-output layers (W_j and b_j) for removal efficiency response (%).

	Input Variables							
	W_{i1}	W_{i2}	W_{i3}	W_{i4}	W_{i5}			
Number of Neurons	**Initial Concentration (mg/l)**	**Adsorbent Dosage (g)**	**Contact Time (min)**	**Temp (ºC)**	**pH**	b_i	W_j	b_j
1	0.9501	-0.5424	-0.6697	-1.2532	-1.1389	-2.395	0.6872	
2	-0.4575	-1.2139	2.0417	1.7252	-1.8339	-1.1357	1.0709	
3	-0.6267	1.5270	0.2842	1.7781	0.79803	-0.0545	0.2270	
4	2.9828	2.0662	-1.7925	-1.0595	3.1654	0.5011	0.8186	
5	-2.3717	0.6959	1.3346	1.8664	-1.5975	0.1560	-0.2548	1.2236
6	-2.2065	0.4832	0.9214	-1.8137	-2.0041	-1.0520	0.0398	
7	-0.9868	0.9382	-0.5830	0.9601	1.1459	-1.4846	-0.1069	
8	-1.0245	0.4299	0.5404	0.5418	2.2036	-1.9841	-0.0093	
9	-0.6984	0.5321	1.1146	-0.6304	2.1565	1.8272	-0.1164	
10	0.3345	-1.7273	-0.5324	-0.9973	-0.8514	2.0075	0.2468	

The Garson's algorithm tipped pH as the most influential factor for the two responses under consideration. As shown in Table 11, the result reveals that the effect follows the order of pH >temperature >contact time >initial concentration > adsorbent dosage for the removal efficiency response while the adsorption amount shows pH > initial concentration > temperature > contact time > adsorbent dosage.

The Olden's algorithm projected initial concentration as the most influential factor among others for both responses and rated initial concentration > contact time > pH > temperature > adsorbent dosage for the removal efficiency of MB on the chitosan flakes. Similarly, for adsorbent amount response, the result records initial concentration > contact time > pH > temperature > adsorbent dosage.

Table 10: Weights and bias in input-hidden layers (W_i and b_i) and hidden-output layers (W_j and b_j) for adsorption amount (mg/g)

Number of Neurons	**Input variables**					b_i	W_j	b_j
	W_{i1}	W_{i2}	W_{i3}	W_{i4}	W_{i5}			
	Initial Concentration (mg/l)	**Adsorbent Dosage (g)**	**Contact Time (min)**	**Temp. (ºC)**	**pH**			
1	1.6045	-0.5689	-0.7389	1.1541	-0.8470	-2.7995	0.5878	
2	0.6920	-1.7025	0.9982	0.8680	0.1741	-2.1378	-0.1907	
3	-1.2276	0.4777	1.2309	0.0583	-1.2136	0.9477	-0.2086	
4	1.2304	-0.1343	0.5546	1.3428	3.1654	-1.3403	0.4218	

5	1.6124	0.5744	-0.0274	-1.0313	-1.5975	-0.1621	0.2888	0.37932
6	-0.4602	0.7017	0.0519	1.4676	1.6757	-0.1334	-0.1845	
7	0.1136	-0.1473	2.0323	0.1720	0.8153	-0.7462	0.0308	
8	-1.7708	0.1880	-0.6075	-1.0412	-0.6464	-1.1341	-0.3673	
9	0.4730	0.5396	-0.8016	-0.8733	-0.8598	2.5783	0.2407	

Table 11: Results of Garson and Olden Algorithm for the percentage removal and Adsorption amount

	Garson Algorithm				**Olden Algorithm**			
	% removal		**q_e (mg/g)**		**% removal**		**q_e (mg/g)**	
Independent Variables	**Relative Importance (%)**	**R**	**Relative Importance (%)**	**R**	**Value**	**R**	**Value**	**R**
Initial concentration (mg/l)	18.32	4	26.31	2	152.80	1	136.23	1
Adsorbent dosage (g)	17.55	5	10.91	5	-18.07	5	-3.434	4
Contact time (min)	19.04	3	13.38	4	-8.621	2	-26.84	5
Temperature (°C)	19.32	2	21.50	3	-14.33	4	31.70	2
pH	25.77	1	27.90	1	-11.78	3	16.04	3

In a similar development, a sensitive analysis (step-by-step approach) was carried out on the independent variable for single and various combinations as shown in Table 12. This kind of sensitivity is a measure of the ANN model on the premises of the mean square error (MSE) and coefficient of determination, R^2. The result the indicates that initial concentration is the most influential input variable among the single combination; initial concentration and contact time were the best among the two factors combined, initial concentration, contact time and pH had the greatest effect among the three factors combination and initial concentration, contact time, temperature and pH had the greatest performance owing to the highest R^2 and the lowest MSE value obtain during the process of neural network optimization topology.

Table 12: Sensitivity analysis for single and various combinations of inputs

S/N	**Input Combination**	**MSE**	**Epochs**	**R2**
1	X_1	8.6584	2	0.7872
2	X_2	23.0140	3	0.2103
3	X_3	20.1040	3	0.3128
4	X_4	21.3037	2	0.3588
5	X_5	21.9248	3	0.2362
6	$X_1 + X_2$	22.4734	5	0.7947
7	$X_1 + X_3$	6.3392	2	0.8471
8	$X_1 + X_4$	8.4868	6	0.7925
9	$X_1 + X_5$	9.1033	3	0.7797
10	$X_2 + X_3$	20.5379	4	0.3190
11	$X_2 + X_4$	19.2197	4	0.3749
12	$X_2 + X_5$	21.9122	4	0.1725

13	X_3+X_4	21.4157	5	0.3421
14	X_3+X_5	19.9778	4	0.3506
15	X_4+X_5	18.3445	3	0.4549
16	$X_1+X_2+X_3$	16.0771	3	0.6560
17	$X_1+X_3+X_4$	4.4831	5	0.8952
18	$X_1+X_4+X_5$	5.9213	4	0.8629
19	$X_2+X_3+X_4$	18.6700	5	0.4049
20	$X_2+X_4+X_5$	24.2263	4	0.3751
21	$X_3+X_4+X_5$	19.1232	5	0.4400
22	$X_1+X_2+X_3+X_4$	6.7782	5	0.8430
23	$X_1+X_3+X_4+X_5$	1.6658	5	0.9635
24	$X_2+X_3+X_4+X_5$	21.7800	6	0.7368

3.5 ANN Empirical formulation equation

From the weights and bias generated, an empirical formula can be developed as adopted by Shahryari et al. [35, 61].

$$Y_r = 0.6872F_1 + 1.0709F_2 + 0.2270F_3 + 0.8186F_4 - 0.2548F_5 + 0.0398F_6 - 0.1069F_7 - 0.0093F_8 - 0.1164F_9 + 0.2468F_{10} + 1.2236 \quad (14)$$

$$Y_q = 0.5878F_1 - 0.1907F_2 - 0.2086F_3 + 0.4218F_4 + 0.2888F_5 - 0.1845F_6 + 0.0308F_7 - 0.3673F_8 + 0.2407F_9 + 0.37932 \quad (15)$$

$$F_i = 2/(1+e^{-2E_i}) - 1,$$

The weighted sum of the input, E_i, is defined as :

$$E_i = w_i \times X_i + b_i$$

Applying the equation to the five process variables under study, the equation becomes:

$$E_i = w_{i1} \times X_1 + w_{i2} \times X_2 + w_{i3} \times X_3 + w_{i4} \times X_4 + w_{i5} X_5 + b_i \quad (16)$$

where Y_r and Y_q represent the empirical equation for percentage removal of MB and the adsorption capacity of the chitosan flakes adsorbent. Also, the coefficients are the weights and biases to the output layer, W_j , i is the number of neurons and F_i is the hyperbolic tangent transfer activation function used in the hidden layer given in equation (5).

3.6 Response Surface Methodology (RSM) AND Artificial Neural Network (ANN) Comparison

Table 13 shows the values of some selected error functions given in equation 17-21 was used in comparing the predicted values with the experimental values for both responses. The results reveal ANN best fits the experimental data because all the statistical indicators produced lower values and higher values of the coefficient of determination, R^2 very close to 1. Table 14 displays the experimental and the predicted values while Figure 19 reveals that the values portrayed a high correlation.

Table 13: Comparison of Error Functions Values of ANN and RSM

Error Function	RSM		ANN	
	Removal Efficiency (%)	Adsorption Amount (mg/g)	Removal Efficiency (%)	Adsorption Amount (mg/g)
MSE	2.4611	0.0036	0.0030	0.0196
ARE	1.5725	0.9780	0.0738	0.7298
EABS	44.0040	1.4942	2.1097	1.1600
ERRSQ	78.7540	0.1166	0.6272	0.0947
R^2	0.8680	0.9988	0.9799	0.9992

Mean Squared Error, MSE:

$$MSE = \frac{1}{n}\sum_{i=1}^{n}\left(Q_{k,\exp t} - Q_{k,pred}\right)^2 \quad (17)$$

Average relative error, ARE:

$$ARE = \frac{100}{N_e}\sum_{k=1}^{N_e}\left|\frac{Q_{k,expt} - Q_{k,pred}}{Q_{k,expt}}\right| \quad (18)$$

Sum of absolute error, EABS:

$$EABS = \sum_{k=1}^{N_p}\left(Q_{k,expt} - Q_{k,pred}\right) \quad (19)$$

Sum of squares of the errors, ERRSQ:

$$ERRSQ = \frac{1}{N_e}\sum_{k=1}^{N_e}\left(Q_{k,expt} - Q_{k,pred}\right)^2 \quad (20)$$

Coefficient of determination, R^2:

$$R^2 = 1 - \frac{\sum_{k=1}^{N_e}\left(Q_{k,expt} - Q_{k,pred}\right)^2}{\sum_{k=1}^{N_e}\left(Q_{k,pred} - Q_e\right)^2} \quad (21)$$

where $Q_{k,expt}$ [$=(q_e)_{k,expt}$ or $(q_t)_{k,expt}$] is the measured adsorption data for run k, $Q_{k,pred}$ [$=(q_e)_{k,pred}$ or $(q_t)_{k,pred}$] the predicted (or calculated) adsorption data for run k, N_e the number of experimental data points and N_p the number of model parameters.

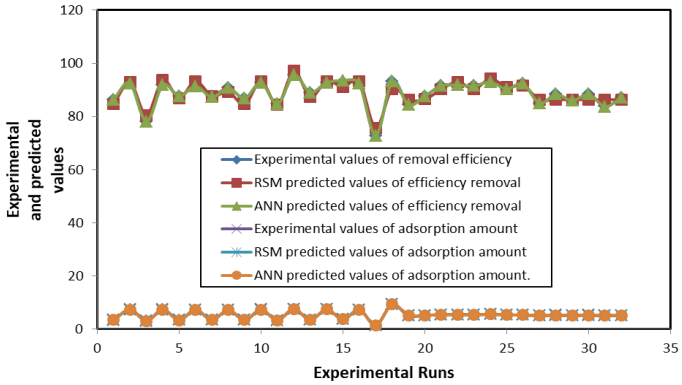

Figure 19: Plot of experimental values and predicted values from RSM and ANN.

3.7 RSM-GA and ANN-GA optimization of process parameters and experimental validation

The process parameter was optimized using the second-order quadratic equation generated (equations 8 and 9) and the empirical function of the Artificial Neural Network tool derived from the weights and bias were used as an objective function where they were optimized using the genetic algorithm tool in a MATLAB environment using the default settings. The objective function was expressed as [27]:

$$y_i = \sum_{j=1}^{n}\left\{ purelin\left[w_{jk} \times \left(\sum_{i=1}^{5}\sum_{j=1}^{n} tansig\left(x_i w_{ik} + b_i \right) \right) \right] + b_j \right\} \quad (22)$$

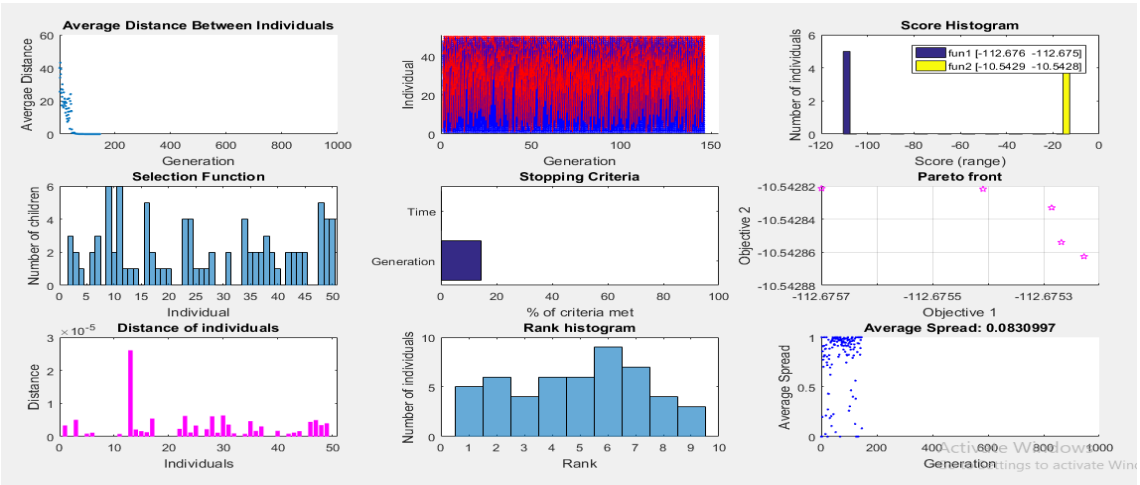

Figure 20: Analysis of the RSM-GA optimization

Table 14. Results of Experimental Values, RSM and ANN predicted percentage removal and Adsorption Capacity.

Experimental Runs (Standard Order)	Experimental Values of Efficiency Removal (%)	RSM- Predicted Values	ANN Predicted values	Experimental Values of Adsorption Amount (mg/g)	RSM-Predicted Values	ANN Predicted values
1	86.4035	84.6365	86.4260	3.4561	3.3882	3.4383
2	92.5439	92.8673	92.5569	7.4035	7.4159	7.3747
3	78.0702	80.5342	78.0767	3.1228	3.2478	3.1404
4	91.8860	93.6740	91.8902	7.3509	7.4159	7.3574
5	87.7193	86.9365	87.7145	3.5088	3.5183	3.4180
6	91.4474	93.3329	91.4459	7.3158	7.3618	7.3040
7	87.7193	87.7432	87.2763	3.5088	3.5183	3.5094
8	90.7895	89.2306	90.7847	7.2632	7.2215	7.2556
9	86.8421	84.6186	86.8114	3.4737	3.4408	3.4731
10	92.7632	93.3177	92.7675	7.4211	7.3984	7.3890
11	84.6491	84.4385	84.6535	3.3860	3.4057	3.3761
12	95.6140	97.1101	95.6153	7.6491	7.6440	7.6407
13	89.0351	87.3869	89.0506	3.5614	3.5007	3.5234
14	92.7632	93.3150	92.7583	7.4211	7.4145	7.4217
15	92.9825	91.1793	93.5384	3.7193	3.7463	3.7257
16	92.3246	93.1349	92.3348	7.3860	7.3794	7.2871
17	72.8070	75.7686	72.7883	1.4561	1.4503	1.4696
18	93.3333	90.3958	93.1059	9.3333	9.3216	9.3600
19	84.5029	86.2878	84.4733	5.0702	5.1645	5.1379
20	87.7193	86.4462	87.7014	5.2632	5.1996	5.2653
21	91.5205	90.2959	91.6075	5.4912	5.4532	5.4261
22	91.8129	93.0615	91.8379	5.5088	5.5292	5.4898
23	91.5205	90.3203	91.5336	5.4912	5.4211	5.4724
24	92.9825	94.2067	92.9970	5.5789	5.6316	5.5761
25	90.3509	91.1054	90.3665	5.4211	5.3860	5.3835
26	92.3041	91.5737	92.2973	5.2982	5.3158	5.2947
27	85.0877	86.3670	84.9960	5.1053	5.1820	5.2107
28	88.3041	86.3670	88.4053	5.2982	5.1820	5.2107
29	85.9649	86.3670	85.9258	5.1579	5.1820	5.2107
30	88.3041	86.3670	88.4053	5.2982	5.1820	5.2107
31	83.9181	86.3670	83.7562	5.0351	5.1820	5.2107
32	87.1345	86.3670	87.1656	5.2281	5.1820	5.2107

The analyses of the optimization process are depicted in Figures 20 and Figure 21 for RSM-GA and ANN-GA respectively. Both figures demonstrate that the iteration terminated after about 50 and 100 generations to achieve the optimum conditions in the design space displayed in Tables 15 and 16, respectively. The validation of predicted optimum conditions (bolden) via experimental works gives 98.96% and 99.28% removal of MB and 9.396 mg/g and 9.259mg/g with an average percentage error of 12.17% and 8.7% respectively for both responses. The result obtained was compared with some previously reported optimized adsorption treatments of MB contaminated aqueous solutions using various adsorbents in Table 17.

Table 15: RSM-GA optimized design space of process variables and corresponding output responses.

	X_1	X_2	X_3	X_4	X_5	Y_{R_e}	Y_{q_e}
1	99.9993	0.2503	18.8584	35.0461	11	112.676	10.5428
2	99.9998	0.2502	18.8596	35.046	11	112.675	10.5429
3	**99.9993**	**0.2502**	**18.859**	**35.046**	**11**	**112.675**	**10.5428**
4	99.9997	0.2502	18.8595	35.046	11	112.675	10.5429
5	99.9997	0.2503	18.8595	35.046	11	112.675	10.5428

Table 16: ANN-GA optimized design space of process variables and corresponding output responses

	X_1	X_2	X_3	X_4	X_5	Y_{R_e}	Y_{q_e}
1	25.6219	0.7713	54.8893	69.8607	7.1345	108.746	10.2918
2	23.2545	0.9706	47.2917	62.6368	8.1945	108.746	10.2918
3	26.0422	0.5429	48.2723	66.1157	10.2079	108.746	10.2918
4	22.2921	0.7648	46.5907	61.7279	7.8162	108.746	10.2918
5	25.6219	0.7713	54.8893	69.8607	6.6345	108.746	10.2918
6	23.2803	0.8758	55.8199	66.5874	7.6417	108.746	10.2918
7	25.8043	0.7592	53.2788	69.3176	7.8559	108.746	10.2918
8	22.2008	0.7457	53.8668	64.1325	7.8016	108.746	10.2918
9	26.379	0.6905	48.9275	71.1786	10.2388	108.746	10.2918
10	30.2017	0.5115	59.4763	74.2352	8.687	108.746	10.2918
11	24.7315	0.8275	48.4216	62.9765	8.2111	108.746	10.2918
12	**25.415**	**0.8572**	**54.1929**	**66.6668**	**8.0327**	**108.746**	**10.2918**
13	24.0261	0.7713	56.101	67.7564	7.8304	108.746	10.2918
14	25.4172	0.7766	55.6923	68.7097	6.9796	108.746	10.2918
15	25.3931	0.7177	51.2046	66.0979	10.1928	108.746	10.2918
16	22.9639	0.6529	62.8682	74.2886	6.8117	108.746	10.2918
17	28.4566	0.6532	54.1605	72.4255	8.5771	108.746	10.2918
18	25.415	0.8569	54.193	66.6669	8.0326	108.746	10.2918

Table 17: Parameters and their optimum conditions of the adsorption of MB by various adsorbents.

S/N	Adsorbent	Mode	Optimization techniques	Parameters	Best optimum conditions	Response value	Reference
1	Tuniks Corm Saffon (Crocus sativas L.)	Batch mode	RSM-Box Behnken Design	Initial concentration, contact time and adsorbent dose.	Adsorbent dose=1.98g/L, contact time=56min and initial concentration= 176mg/L at constant pH value of 5.4 and temperature of 21 ^{o}C.	Percentage removal =89.48%	[45]
2	Defactted Carica papaya seeds	Batch mode	Multi stage batch design	Adsorbent dose, number of adsorption stages and contact time.	Initial concentration= 100mg/L, number of adsorption stage=5 and contact time= 150min.	Percentage removal =99%	[46]
3	Clay minerals	Batch mode	RSM	Initial concentration, contact time and temperature.	Initial concentration=100mg/L, contact time =150min and temperature=60 ^{o}C,	Desorption efficiency =23mg/g	[47]
4	Activated carbon prepared from Bos Indicus Gudali bones	Batch mode	RSM-Box Behnken Design	Intial concentration, adsorbent dose and temperature	Initial concentration=45mg/L, adsorbent dose=0.2g and temperature=60 ^{o}C	Adsorption amount =15.08mg/g	[48]
5	Pine apple bark	Batch mode	RSM-Central Composite Design	Adsorbent dose, temperature and pH	Temperature =30 0C, adsorbent dose=2.5g/L , pH=9.8 for initial concentration of 20mg/L.	Percentage removal =98.91%	[49]
6	Bentonite clay/activated composites	Batch mode	RSM	Temperature, pH and ionic strength	Temperature=40^{o}C	Adsorption capacity= 230mg/g	[50]
7	Chitosan/zeolite composites.	Batch mode	RSM-Central Composite Design.	Contact time, pH adsorbent dose and initial concentration.	Adsorbent dose=2.5g/L, pH=9.0, Initial concentration=43.75mg/L and contact time=138.65 min.	Percentage removal=94%	[26]
8	Pumice	Batch mode	RSM-CCD and ANN-GA	Initial concentration, pH, contact time and adsorbent dose.	Initial concentration=20mg/L, adsorbent dose=1g/L, contact time= 50min and pH=11.	Not reported	[51]
9	Betel Nut Fibre	Batch mode	RSM	Temperature,	Temperature=303K, adsorbent	Adsorption amount	[52]

				adsorbent dose, pH and rotational speed.	dose=15.1g/L, rotational speed=158.5 (rpm) and pH7.5	31.56mg/g	
10	Biochar derived from pomelo peel	Batch mode	RSM and ANN-PSO	Temperature, contact time, initial concentration and pH.	Temperature = 34.63ºC, contact time = 80.00 min, initial MB concentration = 169.73 mg/L and initial pH = 7.	Percentage removal =89.96%	[53]
11	Carboxymethyl cellulose-based hydrogel beads.	Batch mode	RSM	Adsorbent dose, pH and initial concentration.	Adsorbent dosage = 0.6 g Initial concentration= 15 mg/L and pH of 9.5 within contact time of 120 min.	Percentage removal 96.22 $\pm$ 2.96%	[37]
12	DI-Functionalization Activated Carbon	Batch mode	RSM	Adsorbent dose, pH and agitation speed.	Adsorbent dose=4.70g/L, pH=12 and agitation speed=150rpm.	Percentage removal= 95.67%	[58]
13	Dry bean pods husks powder	Batch mode	Taguchi	Initial concentration, adsorbent dose, pH, contact time and temperature.	Initial concentration=50mg/g, adsorbent dose=2.5g/L, pH=10, contact time=30min and temperature=306K.	Percentage removal =87.98%	[54]
14	Bentonite clay	Batch mode	RSM-CCD	Initial concentration, contact time and adsorbent dose	Initial concentration=24.78mg/L, contact time=31.85min and Adsorbent dose=5.25g/L.	99.7%	[55]
15	Polymer Network Hybrid Hydrogel	Batch mode	Taguchi	Initial concentration, adsorbent dose, pH, contact time and temperature.	Initial concentration=10mg/g, adsorbent dose=0.2g/L, temperature=25ºC and pH=9	96.30%	[56]
16	Graphene oxide composites nanoparticles	Batch mode	RSM-BBD	Initial concentration, pH, contact time.	Initial concentration =30ppm, pH= 6.0 and a contact time of 90 min.	99.7%	[57]
17	Activated carbon from agricultural wastes	Batch mode	RSM	Contact time, adsorbent dose and pH.	Not reported	93-99.6%	[80]
18	Physical activated coffe husk	Batch mode	RSM-CCD	Initial concentration, pH	Initial concentration=37.786mg/L,	93.53%	[9]

				and adsorbent dose.	pH=7.637 and adsorbent dose=0.740g		
	Chemical activated coffe husk				Initial concentration=37.786mg/L, pH=7.637 and adsorbent dose=0.740g	92.48%	
19	Graphene oxide/Zinc oxide Nanoparticles.	Batch mode	RSM-BBD	Adsorbent dose, initial concentration, contact time and pH	Adsorbent dose=, initial concentration 5ppm, contact time=8.5min and pH=6	97	[84]
20	Activated carbon derived from millet wood.	Batch mode	RSM-CCD	Initial concentration, contact time, adsorbent dose and pH	Initial concentration=20ppm, contact time=18min, adsorbent dose= 0.2g and pH=7	>99%	[43]
21	Ho-CaWO4	Batch mode	ANN and RSM-CCD	Initial concentration, contact time, adsorbent dose and pH	Initial concentration=100.65mg/L, contact time=15.16min, adsorbent dose=1.91g/L and pH=2.03	71.77%	[44]
22	Activated from *parthenium hysterophorus*	Batch mode	RSM	Initial concentration, temperature, adsorbent dose and pH	Initial concentration=25mg/L, adsorbent dose= 0.22g, temperature=35^{o}C and pH=7	93.4%	[42]
23	Oenological by product	Batch mode	RSM-BBD	Initial concentration, contact time, adsorbent dose and pH	Initial concentration=50mg/L, contact time= 30min, adsorbent dose= 50mg and pH=6	95%	[38]
24	Chitosan prepared from African snail shell	Batch mode	RSM-GA and ANN-GA	Initial concentration, contact time, adsorbent dose, temperature and pH	Initial concentration=25.42mg/L, contact time=54.19min, adsorbent dose=0.86g, temperature= 67^{o}C and pH=8.03	99.28%	This article

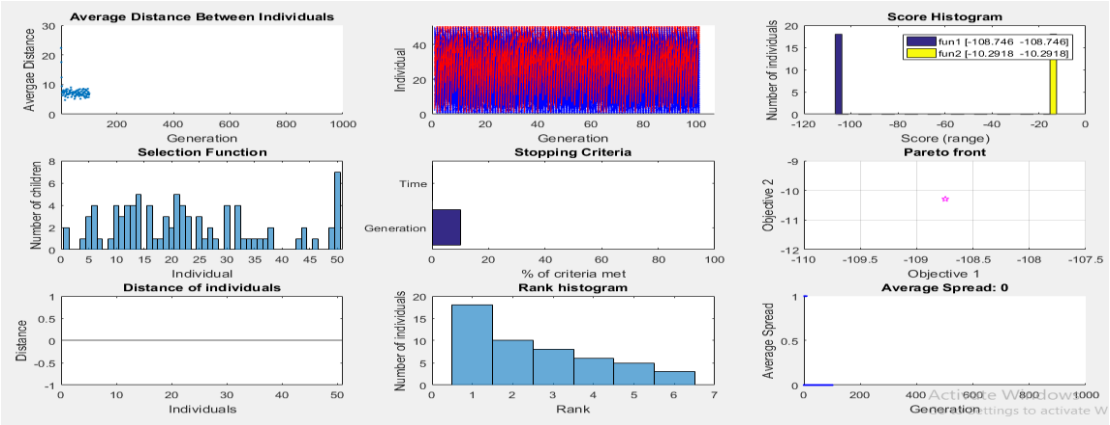

Figure 21: Analysis of the ANN-GA optimization

4. Conclusions

This present study delved into the evaluation of low-cost chitosan adsorbent sourced from African snail shells in the treatment of waste water contaminated with methylene blue dye. The treatment process employed the adsorption process because of its simplicity of operation, relative cost and environmental friendliness. The fractional central composite design based surface response methodology (RSM) characterized by few experimental runs, guarantees good predictive ability and can conveniently accommodate five influential control factors consisting of initial concentration (20-100mg/L), adsorbent dose (0.25-1.25g), contact time (15-75min), temperature (35-95^{o}C) and initial solution pH (3-11) with 5 levels were used to develop the experimental design for appropriate analysis. The analysis covers the analysis of variance (ANOVA), t-test, F test, residual analysis, contour and surface plot. Results of the analysis revealed that at least one single, quadratic and interactive term of the control factors exhibited a high degree of synergetic and antagonistic effects on the response variables. The F test and *p*-value ($p - value < 0.001$) of the model equations for both responses and the non-significance ($p - value > 0.05$) of the lack of fit validate the fitness of the models developed. The relatively high value of R^2 and R^2_{adj} with a difference less than 0.2 within the acceptable limit and Adeq Precision value far greater than 4 for both responses attest more to the model fitness. The elliptical contour shape and curvature of the surface plots depict a high level of interaction of the control factors and a significant impact on the responses. According to the Pareto analysis, initial solution pH, X_5 and adsorbent dosage, X_2 are the most influential parameters for percentage removal and adsorption amount respectively. The artificial neural network (ANN) was used to fit the input-output data of the experimental matrix after achieving the appropriate topology. The R^2 of training (0.979 and 0.999), validation (0.978 and 0.999), test (0.991 and 0.999) and overall (0.980 and 0.999) accordingly for both responses was quite satisfactory. According to Garson's algorithm, initial solution pH was the most influential factor while initial concentration was the most influential parameter for Olden's algorithm and step by step approach while adsorbent dosage was observed to be the factor with the least effect on the response variables for the three sensitivity methods within the purview of this study. The techniques showcased a good predictive ability of the experimental data. However, the ANN technique had the lowest value in all the 5 statistical indices and the highest coefficient of determination, R^2 considered for comparison. Also, the ANN-GA algorithm showed a better performance than the RSM-GA technique in predicting the optimum conditions leading to maximum removal of methylene blue from aqueous solution. The hybrid ANN-GA algorithm produced a better result when compared to previous studies good enough in curbing the negative impact of the effluents from the textile industry on the environment.

References

[1] Mustapha, S., Ndamitso, M.M., Abdulkareem, A.S., Tijani,J.O., Mohammed, A.K. & Shuaib, D.T. (2019). Potential of using Kaolin as natural adsorbent for the removal of pollutants from tannery waste water. *Heliyon*, 5, 1-17. https://doi.org/10.1016/j.heliyon.2019.e02923

[2] Dutta, S., Bhattacharyya, A., Ganguly, A., Gupta, S., & Basu, S. (2011). Application of Response Surface Methodology for Preparation of Low-Cost Adsorbent from Citrus Fruit Peel and for Removal of Methylene Blue. *Desalination*, 275, 26-36 https://doi.org/10.1016/j.desal.2011.02.057

[3] Ebrahimpoor, S. Kiarostami, V., Khosravi, M., Davallo, M. & Ghaedi, A. (2021). Optimization of Tartrazine Adsorption onto Polypyrrole/SrFe12019/Graphene Oxide Nanocomposite Using Central Composite Design and Bat Inspired Algorithm with the aid of Artificial Neural Networks. *Fibers and Polymers*, 22(10), 159-170. http://doi.org/10.1007/s12221-021-8163-9

[4] Ahmed, M. J. (2016). Application of agricultural based activated carbons by microwave and conventional activations for basic dye adsorption. *Journal of Environmental Chemical Engineering*, *4*(1), 89-99. http://dx.doi.org/10.1016/j.jece.2015.10.027

[5] Sahu, N., Rawat, S., Singh, J., Karri, R.R., Lee, S., Choi, J.S. & Koduru, J.R. (2019). Process Optimization and Modeling of Methylene Blue Adsorption Using Zero-Valent Iron Nanoparticles Synthesized from Sweet Lime Pulp. *Applied Sciences*, 9(512), 1-17. DOI: 10.3390/app9235112 http://doi.org/10.3390/app9235112

[6] Chequer, F.M.D., de Oliveira, G.A.R., Ferraz, E.R.A., Cardoso, J.C. Zanoni, M.V.B. & de Oliveira, D.P. (2013). Textile dyes: Dying process and finishing, IntechOpen, London. https://dx.doi.org/10.5772/53659

[7] Slama, H.B., Chenari,B.A., Pourhassan, Z., Alenezi, F.N., Silini, A., Cherif, S.H., Oszako, T. & Luptakova, L. (2021). Diversity of synthetic dyes from the textile industries, discharge impacts and treatment methods. *Applied Science*, 11 (6255), 1-21. https://doi.org/10.3390/app111A6255

[8] Yanto, D.H.Y., Auliana, N., Anita,S.H. & Watanabe, T. (2019). Decolorization of synthetic textile dyes by Laccase from newly isolated trametes hirsata, EDN084 mediated by violuric acid. IOP Conf. Series: Earth and Environmental Science 374, 012005, 1-8. https://doi.org/10.10.88/1755-1315/374/1/012005

[9] Krishna M, T. P., & Gowrishankar, B. S. (2020). Process optimisation of methylene blue sequestration onto physical and chemical treated coffee husk based adsorbent. *SN Applied Sciences*, 2(5). https://doi.org/10.1007/s42452-020-2603-9

[10] Ong, S., Lee, W., Keng, P., Lee, S. & Hung, Y. (2010). Optimization of basic and reactive dye uptakes in binary dye solution using statistical experimental methodology. *International Journal of the Physical Sciences*, 5(14), 2171-2178. ISSN 1992 - 1950

[11] Pereira, L., & Alves, M. (2012). Dyes—environmental impact and remediation. In *Environmental protection strategies for sustainable development* (pp. 111-162). Springer, Dordrecht. Doi:10.1007/978-94-007-1591-2_4

[12] Chequer, F.M.D., de Oliveira, G.A.R., Ferraz, E.R.A., Cardoso, J.C., Zanomi, M.V.B. & de Oliveira, D.P. (2013). Textile Dyes: Dyeing Process and Environmental Impact, Intech, Chapter 6, 151-176. http://dx.doi.org/10.5772/53659

[13] Lellis, B., Polonio, F.Z.C., Pamphile, J.A. & Polonio, J.C. (2019). Effects of textile dyes on health and the environment and bioremediation potential of living organisms. *Biotechnology Research and Innovation*, 3, 275-290. http://doi.org/10.1016/j.biori.2019.09.001

[14] Cifci, D.I., & Meric, S. (2016). Optimization of methylene blue adsorption by pumice powder. *Advances in Environmental Research*, 5(1), 37-50. http://dx.doi.org/10.12989/aer.2016.5.1.037

[15] Corda, N.C., Kini, M. S., Raghuvir, P.B., Mathew, T.M. (2018). A Review on Adsorption of Cationic Dyes using Activated Carbon. MATEC Web of Conferences, 144, 02022, 1-16. http://doi.org/10.1051/matecconf/201814402022

[16] Yusuff, R.O. & Sonibare, J.A. (2004). Characterization of textile industries' effluents in Kaduna, Nigeria and pollution implications. Global Nest: *The International Journal*, 6(3), 212-221.

[17] Durotoye, T.O., Aderonke, A. A., David, O.O. & Onakunle, O. (2018). Impact assessment of waste discharge from a textile industry in Lagos, Nigeria. *Cogent Engineering*, 5, 1531687, 1-11. https://doi.org./10.1080/23311916.2018.1531687

[18] Ajibade, O. M., Banjo, O. A., Oguntuyaki, T. A., Osobamiro, T. M., & Ajakore, A. A. (2020). Implications of carbonates and chlorides contam-ination in groundwater: Examples from textile tie and dye markets in some parts of Southwestern Nigeria. *Indian Journal of Science and Technology*, *13*(32), 3349-3363. https://doi.org/10.17485/IJST/v13i32.539

[19] Awomeso, J.A., Taiwo, A.M., Gbadebo, A.M. and Adenowo, J.A. (2010). Studies on the pollution of waterbody by textile industry effluents in Lagos, Nigeria. *Journal of Applied Sciences in Environmental Sanitation*, 5(4), 353-359. ISSN 0126-2807.

[20] Akintunde, D.G. & Bamgbose, (2020). Seasonal Impact of Ikeja Industrial Wastewaters on water quality of proximate Iya Alaro River in Lagos, Nigeria. *International Journal of Environmental Modelling*, 3(2), 56-67.

[21] Adedeji, O.H. & Olayinka, O.O. (2015). Assessment of ground water contamination by textile effluent discharges in Ikorodu, Nigeria. *Applied Environmental Research*, 37(1), 35-48.

[22] Aneyo, I.A., Doherty, F.V., Adebesin, O.A & Hammed, M.O. (2016). Biodegradation of pollutants in waste water from pharmaceutical , textile and local dye effluent in Lagos, Nigeria. *Journal of Health and Pollution*, 6(12), 34-42. https://doi.org/10.5696/2156-9614-6.12.34

[23] Gerente, C., Lee, V. K. C., Cloirec, P. L. & McKay, G. (2007). Application of Chitosan for the Removal of Metals from Wastewaters by Adsorption—Mechanisms and Models Review. *Critical Reviews in Environmental Science and Technology*, 37(1), 41– 127. http://doi.org/10.1080/10643380600729089

[24] Ozturk, D., Sahan, T. Disu, E.& Aktas, N. (2014). Optimization with response surface methodology (RSM) of adsorption conditions of Cd(II) ions from aqueous solutions by pumice. *Journal of Biology and Chemistry*, 42(2), 183-192. http://doi.org/10.15671/HJBC.20144210857

[25] Amode, J.O., Santos, J.H., Alam, M.Z., Aminul, H.M. & Chan,C.M. (2016). Adsorption of Methylene blue from aqueous solution using untreated and treated (Metroxylon spp.) waste adsorbent: equilibrium and kinetic studies. *International Journal of Industrial Chemistry*, 7, 333-345. http://doi.org/10.1007/s40090-016-0085-9

[26] Dehghani, M. H., Dehghan, A., Alidadi, H., Dolatabadi, M., Mehrabpour, M., & Converti, A. (2017). Removal of methylene blue dye from aqueous solutions by a new chitosan/zeolite composite from shrimp waste: Kinetic and equilibrium study. *Korean Journal of Chemical Engineering*, 34(6), 1699–1707. http://doi.org/10.1007/s11814-017-0077-2

[27] Tsamo, C., Paltahe, A., Fotio, D., Vincent, T. A. & Sales, W. F. (2019). One-, Two-, and Three-Parameter Isotherms, Kinetics, and Thermodynamic Evaluation of Co (II) Removal from Aqueous Solution Using Dead Neem Leaves. *International Journal of Chemical Engineering*, 1–14. http://doi.org/10.1155/2019/6452672

[28] Saleh, T.A. & Gupta, V. K. (2014). Processing methods, characteristics and adsorption behavior of tire derived carbons: A review. *Advances in Colloid and Interface Science*, 211,93-101. http://doi.org/10.1016/j.cis.2014.06.006

[29] Gupta, V. K. Nayak, A. & Agarwal, S (2015). Bioadsorbents for remediation of heavy metals: Current status and their future prospects. *Environmental Engineering Research*, 20(1), 1-18. http://doi.org/10.4491/eer.2015.018

[30] Odoemelam, S. A., Emeh, U. N. & Eddy, N. O. (2018). Experimental and computational chemistry studies on the removal of methylene blue and malachite green dyes from aqueous solution by neem (Azadirachta indica) leaves. *Journal of Taibah University for Science*, 12(3), 255-265. http://doi.org/10.1080/16583655.2018.1465725

[31] Regti, A., El Kassimi, A., Laamari, M. R., & El Haddad, M. (2017). Competitive adsorption and optimization of binary mixture of textile dyes: A factorial design analysis. *Journal of the Association of Arab Universities for Basic and Applied Sciences*, 24(1), 1–9. http://doi.org/10.1016/j.jaubas.2016.07.005

[32] Singh, K. & Arora, S. (2011). Removal of synthetic textile dyes from wastewaters: a critical review on present treatment technologies. *Critical Reviews in Environmental Science and Technology*, 41(9), 807–878. http://doi.org/10.1080/10643380903218376

[33] Olafadehan, O. A., Amoo, K. O., Ajayi, T. O., & Bello, V. E. (2021). Extraction and characterization of chitin and chitosan from Callinectes amnicola and Penaeus notialis shell wastes. *Journal of Chemical Engineering and Material Science*, 12 (12), 1–30. https://doi.org/10.5897/JCEMS2020.0353

[34] Akintunde, D.G. and Bamgbose, (2020). Seasonal impact of Ikeja industrial wastewaters on water quality of proximate Iya Alaro river in Lagos, Nigeria. *International Journal of environmental modelling*, 3(2), 56-67.

[35] Bello, V. E., & Olafadehan, O. A. (2021). Comparative investigation of RSM and ANN for multi response modeling and optimization studies of derived chitosan from Archachatina marginata shell. Alexandria Journal of *Engineering*, 60(4), 3869–3899.https://doi.org/10.1016/j.aej.2021.02.047

[36] Sambo, R. E., Nuhu, A. A. & Uba, S. (2019). Preparation and characterisation of shrimp waste-derived chitin, chitosan and modified chitosan films. *Nigerian Research Journal of Chemical Sciences*, 6, 213-230. http://www.unn.edu.ng/nigerian-research-journal-of-chemical-sciences/

[37] Allouss,D., Essamiali, Y., Amadine, O., Chakir, A.,& Zahouily, M. (2019). Response surface methodology for optimization of methylene blue adsorption onto carboxymethyl cellulose-based hydrogel beads: adsorption, kinetics, isotherm, *Thermodynamics and Reusability Studies. Royal Society of Chemistry Advances*, 9(65), 37858-37869. https://doi.org/10.1039/c9RA06450H

[38] Fouzia, O., Yamina, C., Samia, B. and Zohra, S.A.F. (2022). Three level design to estimate dyes adsorption parameters using oenological by product as adsorbent. *Journal of Environment Treatment Techniques*, 10 (1), 134-142. https://doi.org/10.47277/JETT/10(1)142

[39] Vafakish, B., & Wilson, L. D. (2019). Surface-Modified chitosan: An adsorption study of a "Tweezer-Like" biopolymer with fluorescein. *Surfaces*, *2*(3), 468-484. http://doi.org/10.3390/2030035

[40] Granato, D., & Calado, V.M.A. (2014). *Mathematical and Statistical Methods in Food Science and Technology*, *First edition*, John Wiley and Sons, ltd., 4-17.

[41] Inam, E., Etim, U. J., Akpabio, E. G., & Umoren, S. A. (2017). Process optimization for the application of carbon from plantain peels in dye abstraction. *Journal of Taibah University for Science*, 11(1), 173–185. http://doi.org/10.1016/j.jtusci.2016.01.003

[42] Chatterjee, S., Kumar, A., Basu, S., & Dutta, S. (2012). Application of response surface methodology for methylene blue dye removal from aqueous solution using low cost adsorbent. *Chemical Engineering Journal*, *181*, 289-299. http://doi.org/10.1016/j.cej.2011.11.081

[43] Ghaedi, M.& Kokhdan, S. N. (2015). Removal of methylene blue from aqueous solution by wood millet carbon optimization using response surface methodology. Spectrochimica Acta Part A: Molecular and Biomolecular Spectroscopy, 136, 141–148. http://doi.org/10.1016/j.saa.2014.07.048

[44] Igwegbe, C.A., Mohammadi, L., Ahmadi, S., Rahdar, A., Khadkhodaaiy,D., Dehghami, R., & Rahdar, S. (2019). Modeling of adsorption methylene blue dye on Ho-CaWO4 nanoparticles using response surface methodology (RSM) and artificial neural network (ANN) techniques. Methods X, Vol. 6, 1779-1797. https://doi.org/10.1016/j.mex.2019.07.016

[45] Dbik, A., El Messaoudi, N., Bentahar, S., El Khomri,M., Lacherai, A. and Faska, N. (2022). Optimization of methylene blue adsorption on agricultural solid waste using box-behnken design (BBD) combined with response surface methodology (RSM) modelling. Biointerface Research in Applied Chemistry, 12(4), 4567-4583. https://doi.org/10.33263/BRIAC124.45674583

[46] Unuabonah, E.I., Adie, G.U., Onah, L.O. & Adeyemi, O.G. (2009). Multi-stage optimization of the adsorption of methylene blue dye onto defatted Cariya papaya seeds. *Chemical Engineering Journal*, 155, 567-579. https://doi.org/10.1016/j.cej.2009.07.012

[47] Momina, M.R., Suzylawati, I. & Ahmad, A (2019). Optimization study for the desorption of methylene blue dye from clay based adsorbent coating. *Water*, 11(1304), 1-13. https://doi.org/10.3390/W11061304

[48] Domga, R. Daouda, A., Arnaud, M.A.G., Balike, M., Domga, W.B. & Bosco, I.J. (2022). Optimization of methylene blue adsorption onto activated carbon from Bos Indicus Gudali bones using a box behnken experimental design. American Journal of Chemistry, 12(1), 1-9. https://doi.org/10.5923/j.chemistry.20221201.01

[49] Fegousse, A., El Gaidoumi, A., Miyah, Y., El Mountassir, R. & Lahrichi, A. (2019). Pineapple bark performance in dyes adsorption : optimization by the central composite design. *Journal of Chemistry*, 3017163, 1-11. https://doi.org/10.1155/2019/3017163

[50] Chagas, N.V., Meira, J.S., Anaissi, F.J., Melquiades, F.L., Quinaia, S.P., Felsner,M.L., Justi, R.C. (2014). Preparation, characterization of bentonite clay/activated charcoal composites and 23 factorial design application in adsorption studies of methylene blue dye. *Revista Virtual de Quimica*, 6(6), 1607-1623. https://doi.org/10.5923/1984-6835.20140104

[51] Asgari, G., Darvishmotevalli, M., Beheshti, A., & Salari, M. (2020). Modeling and Optimization of Methylene Blue Adsorption from Aqueous Solution by Pumice Based on RSM-CCD and ANN-GA Methods. *Journal of Environmental Health Enginering*, *8*(1), 83-98. https://jehe.abzums.ac.ir/article-1-808-en.html

[52] Dey, A. K. , & Dey, A. (2021). Selection of Optimal Processing Condition during Removal of Methylene Blue Dye Using Treated Betel Nut Fibre Implementing Desirability Based RSM Approach. In (Ed.), Response Surface Methodology in Engineering Science. IntechOpen. https://doi.org/10.5772/intechopen.98428

[53] Wang, W., Wu, X. & Long, S. (2022). Optimizing the Methylene Blue Removal from Aqueous Solution Using Pomelo Peel Based Biochar Assisted by RSM and ANN-PSO. *Pol. J. Environ. Stud*. 2022;31(1):329–346. https://doi.org/10.15244/pjoes/137947

[54] Mosoarca, G., Popa, S., Vancea, C. & Boran, S. (2021). Optimization,Equilibrium and Kinetic Modeling of Methylene Blue Removal from Aqueous Solutions Using Dry Bean Pods Husks Powder. *Materials* , 14, 5673, 1-14. https://doi.org/10.3390/ma14195673

[55] Savic, I., Gajic, D., Stojiljkovic, S., Savic, I., & Gennaro, S. di. (2014). Modelling and Optimization of Methylene Blue Adsorption from Aqueous Solution Using Bentonite Clay. 24th European Symposium on Computer Aided Process Engineering, 1417–1422. https://doi.org10.1016/b978-0-444-63455-9.50071-4

[56] Yilmaz, E., Guzel Kaya, G., & Deveci, H. (2019). Removal of methylene blue dye from aqueous solution by semi-interpenetrating polymer network hybrid hydrogel: Optimization through Taguchi method. *Journal of Polymer Science Part A: Polymer Chemistry*, 57(10), 1070–1078. https://doi.org10.1002/pola.29361

[57] Archana, B.K.S. Jayanna, A. A., Ananth, M.S, Ali, H.B.A., Muralidhara, K. & Yogesh, K. (2022). Numerical investigations of response surface methodology for organic dye adsorption onto Mg-Al LDH - GO Nano Hybrid: An optimization, kinetics and isothermal studies, *Journal of the Indian Chemical Society*, 99 (1), 100249. https://doi.org/10.1016/j.jics.2021.100249.

[58] Saafie, N., Samsudin, M. F. R., & Sufian, S. (2020). Optimization of Methylene Blue Adsorption via Functionalized Activated Carbon Using Response Surface Methodology with Central Composite Design. *Key Engineering Materials*, 841, 220–224. https://doi.org/10.4028/www.scientific.net/kem.841.220

[59] Pilkington, J.L., Preston, C. & Gomes, R.L.(2014). Comparison of Response Surface Methodology (RSM) and Artificial Neural Network (ANN) Towards Efficient Extraction of Artemisia annua. *Industrial Crops and Products*, 58, 15-24. http://dx.doi.org/10.1016/j.indcrop.2014.03.016

[60] Olden, J. D., Joy, M. K., & Death, R. G. (2004). An accurate comparison of methods for quantifying variable importance in artificial neural networks using simulated data. *Ecological Modelling*, 178(3-4), 389–397. http://doi.org/10.1016/j.ecolmodel.2004.03.013

[61] Shahryari, Z., Sharifi, A., & Mohebbi, A. (2013). Artificial neural network (ANN) approach for modeling and formulation of phenol adsorption onto activated carbon. *Journal of Engineering Thermophysics*, 22(4), 322–336. http://doi.org/10.1134/s181023281304005x

[62] Yu, H.C., Huang, S.M., Lin, W.M., Kuo, C.H., & Shieh, C.J. (2019). Comparison of artificial neural networks and response surface methodology towards an efficient ultrasound-assisted extraction of

chlorogenic acid from *Lonicera Japonica*. *Molecules*, 24(12), 2304. http://doi.org/10.3390/molecules24122304

[63] Sibalija, T.V. (2018). Application of Simulated Annealing in Process Optimization: A Review, Nova Science Publishers, Inc, Chapter 1, 2-49.

[64] Adeyi, A. A., Oloje, A.O., & Giwa, A. (2017) Statistical optimization of chitosan extraction from shrimp shells using response surface methodology. *ABUAD Journal of Engineering Research and Development* (AJERD), 1(1), 8–17.

[65] Zainal, S., Noorul Fhadila, K., Ri Hanum, Y.S., & Rahmah, M. (2014). Optimization of chitosan extract from cockle shell using response surface methodology (RSM). *Asian Journal of Agriculture and Food Science*, 2(4), 1–10. ISSN: 2321 – 1571.

[66] Kalavathy, M.H, Regupathib, I., Pillai, M.G., & Mirandaa, L.R. (2009). Modelling, analysis and optimization of adsorption parameters for H_3PO_4 activated rubber wood sawdust using response surface methodology (RSM). *Colloids and Surfaces B: Biointerfaces*, 70, 35–45. http://doi.org/10.1016/j.colsurfb.2008.12.007

[67] Mourabet, M., El. Rhilassi, A., El Boujaady, H., Bennani-Ziatni, M, El Hamri, R., & Taitai, A. (2012). Removal of Flouride from aqueous solution by Adsorption on Apatitic Tricalcium Phosphate using Box Behnken Design and Desirability Function. *Applied Surface Science*, 258, 4402-4410. https://doi.org/10.1016/j.apsusc.2011.12.125

[68] Bayuo, J., Pelig-Ba, K.B., & Abukari, M.A. (2019). Optimization of Adsorption Parameters for Effective Removal of Lead (II) from Aqueous Solution. *Physical Chemistry: An Indian Journal*, 14 (1), 1-25. www.tsijournals.com

[68] Bhattacharya, Sankha (2021). Central Composite Design for Response Surface Methodology and its Application in Pharmacy.1-19, IntechOpen. http://dx.doi.org/10.5772/intechopen.95835

[69] Olafadehan, A.O., Bello, V.E., Amoo, K.O. & Bello, A.M. (2022). Isotherms, kinetic and thermodynamics studies of methylene blue adsorption on chitosan flakes derived from African giant snail. *African Journal of Environmental Science and Technology*, 16(1), 37-70. https://doi.org/10.5897/AJEST2021.3065

[70] Patel, K. A. & Brahmbhatt, P.K. (2016). A comparative study of the RSM and ANN models for predicting surface roughness in roller burnishing. *Procedia Technology*, 23, 391-397. https://doi.org/10.1016/j.protcy.2016.03.042

[71] Merma, A. G., Olivera, C.A., Hacha, R.R., Torem, M.L. & Santos, B.F. (2019). Optimization of hematite and quartz bioflotation by an artificial neural network (ANN). Journal of mater resource technology, 3, 3076–3087. https://doi.org/10.1016/j.jmrt.2019.02.022

[72] Mourabet, M., El. Rhilassi, A., El Boujaady, H., Bennani-Ziatni, M, El Hamri, R., & Taitai, A. (2012). Removal of Flouride from aqueous solution by Adsorption on Apatitic Tricalcium Phosphate using Box Behnken Design and Desirability Function. *Applied Surface Science*, 258, 4402-4410. https://doi.org/10.1016/j.apsusc.2011.12.125

[73] Awolusi, T. F., Oke, O. L., Akinkurolere, O. O. and Atoyebi, O. D. (2019). Comparison of response surface methodology and hybrid-training approach of artificial neural network in modelling the properties of concrete containing steel fibre extracted from waste tyres, *Cogent Engineering*, 6(1), 1–19. https://dx.doi.org/10.20944/preprints201903.0161.v1

[74] Yulia, F. Chairina, I. Zulys, A. & Nasruddin (2021). Multi-objective genetic algorithm optimization with an artificial neural network for C02/CH4 adsorption prediction in metal-organic frame work. Thermal science and Engineering Progress, 25, 100967. https://doi.org/10.1016/j.tsep.2021.100967

[75] Jafari, M.M., Khayati, G.R., Hosseini, M., Manesh, D.H.(2017). Modelling and optimization roll- binding parameters for band strength of Ti/Cu/Ti clad composites by artificial neural networks and genetic algorithm. *International Journal of Engineering (IJE), Transactions C*, 30, 12, 1885-1893. https://doi.org/10.58.29/ije.2017.30.12c.10

[76] Broujeni, B.R., Nilchi, A.& Azadi, F. (2020). Adsorption modelling and optimization of thorium (iv) ion from aqueous solution using chitosan/TiO2 nano composite: application of artificial neural network and

genetic algorithm. *Environmental Nanotechnology, Monitoring and Management*, 100400. https://doi.org/10.1016/j.enmm.2020.100400

[77] Yao, L., Hong, C. , Dashtiford, H. Esmaeili, H. (2021). Selective removal of sodium ions from aqueous media using effective adsorbents:optimization by RSM and genetic algorithm. *Acta Chim Slov*., 68 (4), 791-803. https://doi.org/10.17344/acsi.2021.6762

[78] Hamidi, F., Dehgham, M.H., Kasraee, M., Salari, M., Shiri, L. & Mahvi, A.H. (2022). Acid red18 removal from aqueous solution by new crystalline granular ferric hydroxide (GFH): optimization by response surface methodology and genetic algorithm. *Scientific Report*, 12(4761), 1-15. https://doi.org/10.1038/s41598-022-08769

[79] Deng, S. & Chen, Y. (2019). A study by response surface methodology (RSM) on optimization of phosphorus adsorption with nano-spherical calcium carbonate derived from waste. *Water Science & Technology*, 79(1), 188-197.https://iwaponline.com/wst/article-pdf/79/1/188/663919/wst079010188.pdf

[80] Ali, A.F., Kovo, A.S. and Adetunji, S.A. (2017). Methylene blue and brilliant green dyes removal from aqueous solution using agricultural wastes activated. *Journal of Encapsulation and Adsorption Sciences*, 7, 95-107. https://doi.org/10.4236/jras.2017.72007

[81] Saini, S. Chawla, J., Kumar, R. & Kaur, I.(2019). Response surface methodology (RSM) for optimization of cadmium ions adsorption using $C_{16\text{-}6\text{-}16}$ incorporated mesoporous MCM-41. *SN Applied Sciences*, 1, 894-904. https://doi.org/10.1007/s42452-019-0922-5.

[82] Ghogomu, J. N., Noufame, T. D., Ketcha, M. J. & Ndi, N. J. (2013). Removal of Pb (II) ions from aqueous solutions by kaolinite and metakaolinite materials. *British Journal of Applied Science & Technology*, 3, Issue 4, 942–961. http://dx.doi.org/10.9734/BJAST/2013/4384

[83] Tolcha, T., Gemechu, T., & Megersa, N. (2020). Flower of Typha latifolia as a low-cost adsorbent for quantitative uptake of multiclass pesticide residues from contaminated waters. *South African Journal of Chemistry*, *73*, 22-29 https://doi.org/10.17159/0379-4350/2020/v73a4

[84] Hosseini, S.A., Mashayki, S & Babaei, S. (2016). Graphene Oxide/ Zinc Oxide nanocomposites: A superior adsorbent for removal of methylene blue-statistical analysis by response surface methodology (RSM). *South African Journal of Chemistry*, 69, 105-112.

[85] Chittoo, B. S. & Sutherland, C. (2019). Adsorption Using Lime-Iron Sludge–Encapsulated Calcium Alginate Beads for Phosphate Recovery with ANN- and RSM-Optimized Encapsulation. *Journal of Environmental Engineering*, 145(5), 04019019. doi:10.1061/(asce)ee.1943-7870.0001519

[86] Supeni, E.E., Eparachchi, J.A., Islam, M.M. & Lau, K.T.(2013). Development of artificial neural network model in predicting performance of smart wind turbine blade. 3rd Malaysian postgraduate conference (MPC 2013), 233-242.

[87] Wang, Q. L., Apul, O. G., Xuan, P., Luo, F. & Karanfil, T. (2013). Development of a 3DQSPR model for adsorption of aromatic compounds by carbon nanotubes: comparison of multiple linear regression, artificial neural network and support vector machine. *RSC Advances*, 3(46), 1-32. http://doi.org/10.1039/c3ra43599g

[88] Lee, J., Kim, C.G., Lee, J., Kim, N. and Kim, H. (2018). Application of Artificial Neural Networks to Rainfall Forecasting in the Geum River Basin, Korea. *Water*, 10 (10), 1448. http://doi.org/10.3390/w10101448

[89] Hamidi, F., Dehgham, M.H., Kasraee, M., Salari, M., Shiri, L. & Mahvi, A.H. (2022). Acid red18 removal from aqueous solution by new crystalline granular ferric hydroxide (GFH): optimization by response surface methodology and genetic algorithm. *Scientific Report*, 12(4761), 1-15. https://doi.org/10.1038/s41598-022-08769